Stratigraphy and Geological Correlation, Vol. 13, No. 1, 2005, pp. 1–20. Translated from Stratigrafiya. Geologicheskaya Korrelyatsiya, Vol. 13, No. 1, 2005, pp. 3–25.

Metasedimentary Complexes of the Tuva–Mongolian Massif: Age, Provenances, and Tectonic Position

I. K. Kozakov*, E. B. Sal'nikova*, A. Natman, V. P. Kovach*, A. B. Kotov*, V. N. Podkovyrov*, and Yu. V. Plotkina***

**Institute of Precambrian Geology and Geochronology, Russian Academy of Sciences, nab. Makarova 2, St. Petersburg, 199034 Russia*

***Research Center of Earth Sciences, National University of Australia, Canberra ACT 0200, Australia*

Received February 8, 2004; in final form, April 14, 2004

Abstract—A complex problem of dating supracrustal rocks is unavoidable by analysis of tectonic position of polymetamorphic amphibolite and granulite complexes. Geochronological dates are necessary to constrain ages of source rocks and accumulation periods of clastic sediments, while isotopic-geochemical parameters open a possibility to estimate model ages of the crust in provenances. Using the ion microprobe SHRIMP^{TM} (Hiroshima, Japan), clastic zircons from metasediments of the Erzin and Moren complexes of the Tuva–Mongolian massif in accretionary collage of Central Asia are dated and the Nd model age of respective rocks are estimated. The U–Th–Pb isotopic data suggest that clastic zircons from supracrustal complexes of the Tuva–Mongolian massif were derived from the Late Riphean rocks 0.70 to 0.90 Ga old. The upper age limit is determined by synmetamorphic granitoid intrusions 536 ± 6 Ma old, and stratigraphic range of the complexes presumably corresponds to the terminal Upper Riphean–Vendian. The Early Riphean (1.4–1.5 Ga) and pre-Riphean (1.9 and 2.56 Ga) dates that are established in particular cases characterize most likely the ages of rock complexes in provenances of classic sediments. To the first approximation, the accumulation period of protoliths for gneiss–migmatitic complexes of the Tuva-Mongolian massif is correlative with the incipient breakup of Rodinia (~730 Ma ago) and opening of Vendian oceans. Accumulation of respective sediments in settings of a passive continental margin was connected with erosion of volcano–plutonic rock associations formed before the Rodinia breakup and at the commencement of this event. It is possible to assume that margins of Rodinia experienced rifting with breakout of their fragments 1.0–0.73 Ga ago, whereas formation of volcanic arcs and islands was in progress within the ocean surrounding that supercontinent. In the terminal Late Riphean and Vendian, rocks originated at that time and products of their destruction formed the basement beneath terrigenous and carbonate sediments of microcontinents, the Tuva–Mongolian massif included.

Key words: geochronology, zircons, Nd isotope systematics, Vendian, Riphean, Rodinia, Paleo-Asian ocean, Tuva–Mongolian massif.

INTRODUCTION

By analogy with crystalline basement rocks of ancient platforms, some structural–lithologic complexes of Phanerozoic foldbelts, e.g., crystalline rocks of amphibolite and especially granulite metamorphic facies, are attributed to the Lower Precambrian. In the Siberian platform southern fringe, the highly metamorphosed supracrustal rocks are widespread in Caledonian foldbelts and in the Dzabkhan and Tuva–Mongolian massifs or microcontinents (Fig. 1). Tectonic interpretation of the latter is controversial. Originally, the Tuva-Mongolian massif was regarded as a structure with the Early Precambrian basement within the southern Paleozoic fringe of Siberian platform (*Tectonic Map…*, 1979; Il'in, 1982; Fedorovskii *et al.*, 1995). Crystalline complexes of the Sangilen Upland, northern Mongolia, southeastern West Sayan Mountains, and western Khamar–Daban Ridge were attributed to this structure. Il'in (1982) connected formation of the Tuva-Mongolian massif with evolution of the Late Riphean–Cambrian continental margin of Siberian craton. He distinguished three structural complexes of that margin: the pre-Upper Riphean crystalline basement, Upper Riphean rift complex, and Vendian–Cambrian cover of carbonate shelf deposits. Almost all the highly metamorphosed rocks southward of the Siberian platform were attributed to the massif (Il'in, 1982). Later on, Belichenko and Boos (1988) suggested that metamorphic complexes of the Khamar-Daban Ridge, rocks of the granulite facies included, originated during evolution of the Caledonian mobile belt fringing the Bokson–Khubsugul–Dzabkhan microcontinent as it was called. The microcontinent included the Gargan block, Sangilen massif, and crystalline complexes of central and northern Mongolia (*Early Precambrian…*, 1993). Gneiss–migmatitic polymetamorphic complexes of the Gargan block, western Tuva–Mongolian massif, and Baidarik block were attributed to presumably the pre-

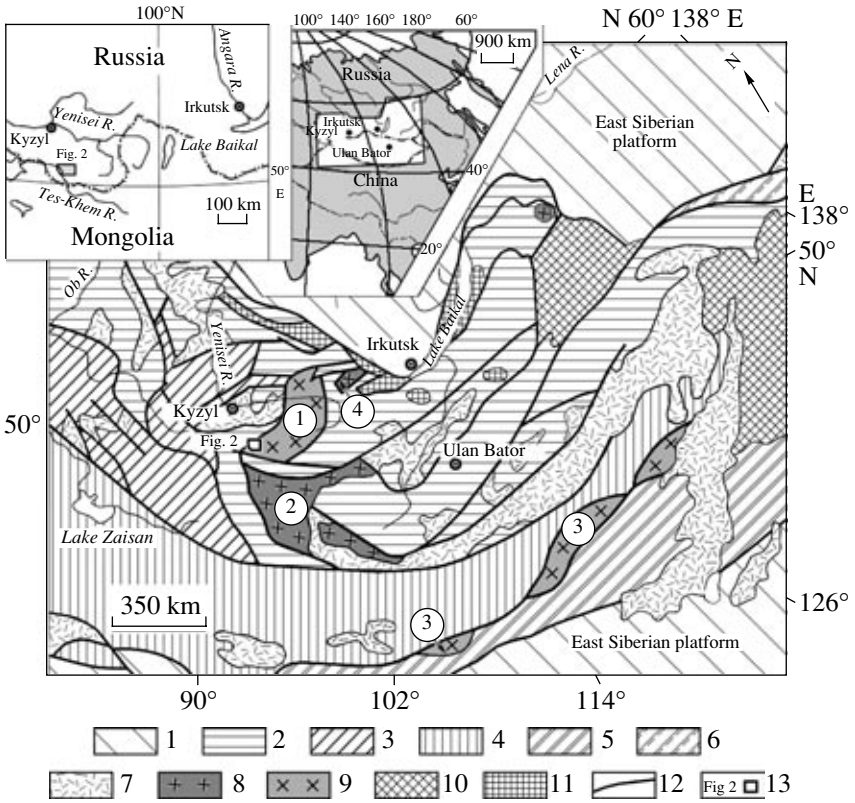

Fig. 1. Tectonic scheme of Central Asia (after *Tectonic Map…*, 1978, and Mossakovskii *et al.*, 1993, with modifications): (1) ancient platforms; (2) Neoproterozoic to Early Paleozoic and (3) Middle Paleozoic structures of accretionary type; (4) Late Paleozoic, (5) Early and (6) Late Mesozoic structures of collision type; (7) Phanerozoic volcanic belts; (8–10) continental blocks with pre-Riphean (8), Riphean (9) and problematic (10) ages of basement; (11) metamorphic complexes of Early Caledonian accretionary collage; (12) main tectonic boundaries; (13) position of West Sangilen area (Fig. 2) in the inset map.

Riphean basement of the microcontinent (Fig. 1). Rock of the Archean age are not established elsewhere except for the Dzabkhan massif (Kozakov *et al.*, 1997a) and Gargan block (our unpublished data).

Recent geological, geochronological, and isotopic-geochemical investigations (Kozakov *et al.*, 1999, 2001) showed that the Tuva-Mongolian massif is a heterogeneous structure but not the indivisible microcontinent with the pre-Riphean basement. During the Early Caledonian tectogenesis, it successively amalgamated rock complexes of different age and origin: fragments of microcontinents with pre-Riphean basement (Gargan block) and fragments of shelf, island arcs, and oceanic crust of Late Riphean to Vendian ages (Yarmolyuk *et al.*, 1999; Kozakov *et al.*, 2001). As was shown therewith, polymetamorphic Erzin and Moren complexes formerly attributed to the basement of microcontinent (Mitrofanov *et al.*, 1981; Kozakov, 1986) originated during the development of the Early Caledonian metamorphic zoning (Kozakov *et al.*, 1999; Kotov *et al.*, 1997). Nevertheless, the problem of geochronology and tectonic position of the highly metamorphosed supracrustal rocks of the Tuva-Mongolian massif remained unsolved. Until recently, the basement rocks of the Tuva-Mongolian massif were interpreted to be of Early Precambrian age and the massif itself was regarded as a fragment of an ancient craton. Some researchers assumed that the massif was split off the eastern Gondwana in the terminal Late Proterozoic and then was docked to accretionary collage fringing the Siberian craton in the course of tectonic evolution of the Paleo-Asian ocean (Mossakovskii *et al.*, 1993; Didenko *et al.*, 1994). In opinion of other geologists, the Gargan block, Tuva-Mongolian massif, and Dzabkhan microcontinent (Fig. 1) represent an integral continental mass split of Siberian craton in the Riphean time (Berzin *et al.*, 1994). In some tectonic schemes, the Tuva-Mongolian massif and Gargan block are attributed to different systems of microcontinents (Mossakovskii *et al.*, 1993; Didenko *et al.*, 1994). The alternative viewpoint is based on Middle and Early Riphean Sm–Nd model ages of the Paleozoic granitoids of the Tuva-Mongolian massif (Kozakov *et al.*, 1997b) and presumes that the massif basement is composed of the Early–Middle Riphean island-arc complexes (Kovalenko *et al.*, 1999; Yarmolyuk *et al.*, 1999).

According to biostratigraphic and geochemical data, there are two age horizons in the carbonate cover of the Bokson–Khubsugul–Dzabkhan microcontinent (Belichenko *et al.*, 1999; Letnikova, 2002). Shallow-

sea dolostones of the older level (Irkut Formation) discordantly overlie crystalline basement of the Gargan block along its periphery. The Sumsunur granitoids that intruded these dolostones yield zircons with U–Pb ages of 785 ± 11 Ma, and this date constrains the upper age limit of their host sediments (Kuzmichev *et al.*, 2000). Shallow-sea carbonates of the younger, much more widespread level correspond to the stage of carbonate platform development above the Tuva-Mongolian massif (Il'in, 1982; Belichenko *et al.*, 1988; Kuzmichev, 1994, 2001; Kuzmichev *et al.*, 2001). Basal interval of these rocks is estimated to be ranging in age from the Late Riphean to Early Cambrian. In southeastern areas of the East Sayan Mountains, for instance in the Bokson–Sarkhoi depression, basal siliciclastic beds of the Bokson Group yield the Late Vendian microfossils (Veis and Vorob'eva, 1993), and lower carbonate strata of the group host the Vendian (Yudomian) stromatolites (Semikhatov and Serebryakov, 1967). The younger carbonate level is distinguished at the north and south parts of the Tuva-Mongolian massif. In northern areas of the Tuva-Mongolian massif, the Vendian–Cambrian carbonate succession discordantly rests on different Upper Riphean strata (Kuzmichev, 1994). In southern areas of the massif (West Sangilen Upland), carbonate and siliciclastic–carbonate deposits of the second level were attributed to the Balyktygkhem, Chartiss, and Naryn formations (Il'in, 1958). There was suspected stratigraphic unconformity between the Chartiss and Naryn formations, and Vendian age of the latter was inferred based on microphytoliths occurring in the carbonate strata (Aleksandrov, 1991; Gonikberg, 1997) and black shale member of the formation (Mal'tsev and Mezhelovskii, 1967). According to above data, the Balyktygkhem and Chartiss formations were attributed to the Lower Proterozoic (Mitrofanov *et al.*, 1981). When conformable relations between the Naryn and Chartiss formations were substantiated later on, the succession of Balyktygkhem, Chartiss, and Naryn formations was termed the Sangilen Group (Gibsher and Terleev, 1989; Gibsher *et al.*, 1987) or Naryn Complex (Kozakov *et al.*, 1999, 2001). In addition to carbonate successions, the Naryn Complex includes quartzites and schists of the Chinchilig Formation, which are products of the regional metamorphism in the Erzin–Chinchilig interfluve (Kozakov *et al.*, 1999). The low-grade metamorphism that affected the Moren Complex by the end of the Vendian (536 ± 6 Ma ago) is untypical of the Naryn Complex. Accordingly, it was assumed that rocks of both complexes were set apart until the terminal Vendian and became conjugate in response to the Middle or Late Cambrian tectonic events (Kozakov *et al.*, 2001).

In this work, we report the results of SHRIMP™ detrital zircon dating and Nd isotopic systematics for metasedimentary rocks of the Erzin and Moren complexes of the southwestern Tuva–Mongolian massif. Along with geological, geochronological, and isotopic-geochemical data on magmatic rocks of the massif (Kozakov *et al.*, 2003), the results obtained offer a possibility to assess ages of rocks from both complexes and to determine provenances and source rocks of clastic material. Finally, geological development of the Tuva-Mongolian massif is reconsidered in terms of general geodynamic model of the Early Caledonian accretion in central Asia.

METAMORPHIC COMPLEXES OF THE TUVA-MONGOLIAN MASSIF

Metamorphic complexes under discussion are well represented in western structures of the Tuva-Mongolian massif, i.e., in the Western Sangilen and in the northern flank of the Han-Huhei Range (Kozakov, 1986). They are of different composition, origin, and metamorphic history. The Erzin and Moren complexes of gneissic and migmatitic rocks are of polymetamorphic origin, while the Naryn Complex includes carbonate, siliciclastic–carbonate, and siliciclastic successions once metamorphosed under conditions of greenschist to amphibolite facies (Fig. 2). In contrast to polymetamorphic gneissic and migmatitic rocks formerly attributed to the basement of Tuva–Mongolian massif, metasedimentary rocks of the Naryn Complex were included into the upper structural unit (Il'in, 1982; Mitrofanov *et al.*, 1981; Gibsher *et al.*, 1989; Gonikberg, 1997; Belichenko *et al.*, 1999). Age relations between the above metamorphic complexes cannot be inferred from geological observations, because structural plan in western areas of the massif is determined by a system of tectonic slices different in age and thickness, which are composed of rocks of the Erzin, Moren, and Naryn complexes. Rock associations of individual tectonic slices can be regarded only as fragments of former successions.

We present below only brief information on metamorphic complexes, because tectonic settings of their formation have been reconstructed based on petrochemical data and properly discussed in a series of publications (Mitrofanov *et al.*, 1981; Kozakov, 1986; *Early Precambrian…*, 1993). Original composition of metamorphosed sedimentary, volcanogenic-sedimentary, and volcanic rocks is established with the help of classification diagrams plotted by Neelov (1980). With respect to formation settings of metamorphic rocks in the Western Sangilen, our conclusions are consistent with results of Gonikberg (1997) who determined protoliths of metasedimentary rocks using the diagram of Rozen (1993).

The Moren Complex includes two rock associations of volcanic and sedimentary rocks, which were twice metamorphosed under conditions of low- and high-pressure amphibolite facies. One association is mostly represented by biotite, garnet–biotite (±disthene), and two-mica gneisses, while the other one consists of similar gneisses associated with marbles, quartzites, and subordinate amphibolites. In many cases, amphibolites correspond to deformed and meta-

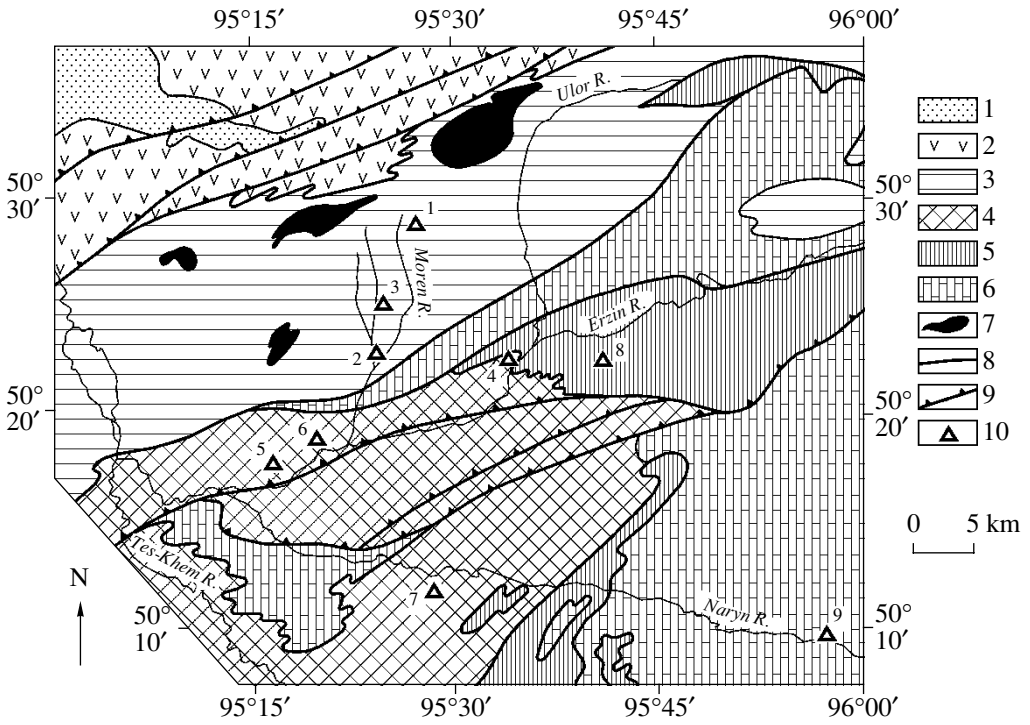

Fig. 2. Geological scheme of Western Sangilen: (1) Devonian deposits; (2) ophiolites of the Early Caledonian Agardag–Erzin zone; (3) Moren and (4) Erzin polymetamorphic complexes; (5) terrigenous and (6) carbonate–terrigenous metasediments of Naryn Complex; (7) ultramafic rocks; (8) faults; (9) thrust faults; (10) sampling sites by ordinal numbers as in Tables 1 and 4.

morphosed basic dikes, which intruded rocks of the complex between two stages of metamorphism (Kozakov, 1986; Kozakov *et al.*, 1999). Despite the conformable relations with enclosing gneisses, these orthoamphibolites prevailing in the complex are excluded from consideration of the original sedimentary succession. Sediments ranging in composition from ferruginous oligomictic and quartz sandstones to graywackes are reconstructed as protoliths of gneisses from the first association. Gneisses of the second association correspond to metamorphosed oligomictic to polymictic sandstones, siliciliths, and volcanics of the rhyolite–dacite series. In general, it is possible to assume that protoliths of metamorphic rocks of the Moren Complex were deposited in rift structures of passive continental margins (Kozakov, 1986; *Early Precambrian…,* 1993; Gonikberg, 1997).

The Erzin Complex is represented by biotite and garnet–biotite gneisses of amphibolite facies, which are intensively migmatized and retain relicts of granulites. The latter correspond in composition to hypersthene, hypersthene–garnet–biotite, two-pyroxene, spinel–garnet–biotite, and sillimanite–cordierite gneisses. Their protoliths were various sedimentary rocks: quartzites, arkosic sandstones, hydromica pelites with moderate alumina content, and calcareous shales. A high maturity of sediments, metamorphic equivalents of which prevail in the Erzin Complex, suggests stable tectonic environments of sedimentation, which are characteristic of sedimentary basins in passive continental margins.

The Naryn Complex includes rocks of the greenschist to amphibolite facies. These are metamorphosed carbonate, siliciclastic–carbonate, and siliciclastic deposits of the Balyktygkhem, Chartiss, Naryn, and Nizhnii Naryn formations. Terrigenous metasediments of the Chinchilig Formation, i.e., biotite or two-mica quartzose schists and garnet–biotite gneisses of the Erzin–Chinchilig drainage-divide area (Fig. 2), which originated after arkosic to greywacke sandstones and K–Na pelites, are also attributed to the Naryn Complex. Gonikberg (1997) who studied geochemistry of carbonate succession in the Western Sangilen showed that it corresponds in composition to marl–limestone formations of epicontinental seas and passive margins. As is suggested, the succession was deposited either in deep distal settings of a broad shelf, or in carbonate platforms split off the shelf (Gonikberg, 1997).

ANALYTICAL PROCEDURE

X-ray fluorescence spectroscopy and ICP-MS method were used to analyze respectively the major elements and REE with a relative error of 5 to 10%. Geochronology of detrital zircons was studied using the ion microprobe SHRIMP^{TM} II (Hiroshima, Japan) and technique described earlier (Compston *et al.*, 1984; Roddick and van Breemen, 1994; Claoué-Long *et al.*,

Table 1. Chemical composition of type metamorphic rocks from the Tuva–Mongolian massif (wt %)

No.	Sample no.	SiO_2	TiO_2	Al_2O_3	Fe_2O_3	FeO	MnO	MgO	CaO	Na_2O	K_2O	P_2O_5	H_2O	Sum
Moren Complex														
1	5613	68.00	1.11	14.88	5.26*		0.07	3.06	1.91	2.00	2.93	0.08	0.00	99.48
2	5741	69.40	0.83	12.90	2.20	3.40	0.37	2.20	2.60	2.20	2.50	0.11	0.98	99.60
3	5558-1	65.89	0.72	15.54	6.28*		0.09	3.02	1.91	2.36	3.52	0.16	0.00	99.99
Erzin Complex														
4	5616	56.00	1.50	22.00	1.60	8.40	0.36	5.40	0.26	0.48	1.40	0.05	2.40	99.80
5	5617	71.50	0.79	14.40	1.40	2.10	0.44	1.50	4.20	2.10	0.85	0.05	0.62	99.80
6	5525	62.10	1.00	17.80	2.20	4.30	0.09	1.90	0.98	2.10	4.30	0.12	2.70	99.60
7	5546	57.29	0.30	14.09	4.7*		0.30	4.06	16.14	0.23	0.40	0.34	1.90	99.75
Naryn Complex														
8	5740	79.20	0.26	10.70	2.00	1.00	0.01	1.10	0.30	1.20	2.60	0.07	1.50	99.80
9	5553	65.41	0.26	15.5	4.84*		0.05	3.01	2.39	3.84	3.36	0.25	0.29	99.82

Note: (5613) disthene–garnet–biotite gneiss; (5741) garnet–biotite gneiss; (5558-1) biotite gneiss; (5616) spinel–sillimanite–cordierite gneiss; (5617) two-pyroxene gneiss; (5525) sillimanite–cordierite gneiss; (5546) hypersthene gneiss; (5740) two-mica schists from succession of terrigenous metasediments; (5553) biotite gneiss from interlayer in marbles of the Naryn Complex (*total iron as Fe_2O_3).

1995). Measured isotopic ratios are normalized to parameters of the zircon standard SL13 from the University of Australia (572 Ma, $^{206}Pb/^{238}U = 0.0928$). The uncertainty values are given at 2σ level. Correction for common lead corresponds to the published model values (Cumming and Richards, 1975). Standard decay constants of U (Steiger and Jager, 1976) are used in age calculations.

The Nd isotopic analyses are performed in accord with method described by Kotov *et al.* (1995). Total blank during the period of measurements was 0.03–0.2 ng for Sm and 0.1–0.5 ng for Nd. Measured $^{143}Nd/^{144}Nd$ ratios are normalized to $^{146}Nd/^{144}Nd = 0.7219$ and corrected for $^{143}Nd/^{144}Nd = 0.511860$ characterizing the La Jolla standard. The measurement accuracy is ±5% (2σ) for Sm and Nd concentrations, ±0.5% for $^{147}Sm/^{144}Nd$ ratio, and ±0.005% for $^{143}Nd/^{144}Nd$ ratio. The weighted mean for 13 measurements of $^{143}Nd/^{144}Nd$ ratio in the La Jolla standard is 0.511839 ± 7 (2σ). Parameters $\varepsilon_{Nd}(0)$ and model ages $T_{Nd}(DM)$ are calculated using values $^{143}Nd/^{144}Nd = 0.512638$, $^{147}Sm/^{144}Nd = 0.1967$ in CHUR (Jacobsen and Wasserburg, 1984) and $^{143}Nd/^{144}Nd = 0.513151$, $^{147}Sm/^{144}Nd = 0.2136$ in DM (Goldstein and Jacobsen, 1988). Because of possible fractionation of Sm and Nd during erosion, sedimentation, and metamorphism, we calculated model ages $T_{Nd}(DM)$ and $T_{Nd}(DM\text{-}2st)$ for one- and two-stage models (Keto and Jacobsen, 1987).

GEOCHEMICAL CONSTRAINTS

Considered below are data on chemical composition and trace element distribution in representative rock samples from the Moren and Erzin complexes (Tables 1, 2; Fig. 3), which have been subjected to U–Th–Pb geochronological and Nd isotopic analysis, and on metasediments of the Naryn Complex. Sampling sites are shown in Fig. 2.

Moren Complex. Prevailing among protoliths of the Moren Complex are K–Na polymictic to subgraywacke magnesian (2.2–3.06 MgO) and ferruginous (5.26–6.28% Fe-oxides in sum) sandstones (Table 1). Garnet–disthene–biotite gneisses of the complex (polymictic metasandstone, Sample 5613, Table 2) are somewhat enriched in Rb, Sr, and Ba relative to the typical tonalite (Taylor and McLennan, 1985). Simultaneously, they show higher ratios $(La/Yb)_N = 10.6$ and $La/Sc = 3.2$ (Table 2, Fig. 3), but lower ratios $Eu/Eu^* = 0.57$ and $Th/Sc = 0.70$. These parameters imply that gneisses originated after sediments, clastic material of which was derived from crustal granitoids and metamorphic rocks with La/Sc = 0.7–27 and Th/Sc = 0.64–18, on the one hand, and from basic to intermediate volcanics with La/Sc = 0.4–1.1 and Th/Sc = 0.05–0.4, on the other (Cullers, 2000). Judging from REE spectrum and distinct Eu-anomaly (Sample 5613, Table 2), contribution of crustal material was more significant than that of andesite–basaltic volcanics. Based on petrochemical classification of Neelov (1980), we suspect source rocks of similar composition for protoliths of biotite gneisses in the Moren Complex, which corresponded to polymictic (Sample 5741) and subgraywacke sandstones (Sample 5558-1, Table 1).

Erzin Complex. Petrochemical and geochemical data on representative gneiss samples from the Erzin Complex also suggest different source rocks of clastic material in their protolith. Spinel–sillimanite–cordierite gneisses (Sample 5619, Table 1) are comparable in chemical composition with kaolin–hydromica shales. The negative Eu-anomaly ($Eu/Eu^* = 0.62$) characteriz-

Table 2. Concentration of trace elements in type metamorphic rocks from the Tuva–Mongolian massif (ppm)

Sample no.	5613	5616	5616a	5617	5740
Ba	1056	547	528	638	632
Sr	182	96	94	494	84
Rb	90	52	50	53	39
Th	9.1	9.9	9.3	8.2	3.7
Sc	13.0	35.7	35.0	13.4	4.6
La	42.1	24.1	23.0	27.9	11.5
Ce	87.0	50.7	47.7	55.5	24.5
Pr	10.9	5.9	5.67	6.29	2.94
Nd	39.7	20.3	10.6	39.7	20.9
Sm	7.9	3.77	3.48	4.21	1.84
Eu	1.49	0.83	0.79	1.23	0.59
Gd	7.77	4.16	3.92	3.8	1.64
Tb	1.09	0.71	0.66	0.50	0.22
Dy	5.45	5.33	5.39	3.04	1.34
Ho	1.00	1.32	1.33	0.60	0.24
Er	2.73	4.66	4.66	1.79	0.72
Tm	0.44	0.81	0.84	0.27	0.11
Yb	2.68	5.9	6.03	1.58	0.78
Lu	0.38	0.98	0.94	0.24	0.12
Eu/Eu*	0.57	0.61	0.62	0.94	1.02
$(La/Yb)_N$	10.6	2.8	2.6	11.9	9.9
La/Sc	3.24	0.68	0.66	2.08	2.5
Th/Sc	0.70	0.28	0.27	0.61	0.80

Note: Rock types as in Table 1; 5516 and 5516a duplicate analyses of one sample.

ing REE spectrum in these rocks and high Zr concentration used to be considered as indicators of sedimentary material recycling (McLennan *et al.*, 1993). According to elevated FeO (8.4%) and MgO (5.4%, Table 1) contents associated with low ratios $(La/Yb)_N$ = 2.6, La/Sc = 0.66, and Th/Sc = 0.28 (Table 2), which are characteristic of provenances with prevailing mafic rocks, protoliths of above gneisses consisted mostly of clasts derived from basic magmatic rocks. At the same time, sillimanite–cordierite gneisses of the Erzin Complex (Sample 5525) correspond in chemical composition to hydromica shales of the platform weathering profiles connected with provenances, which are composed of silicic magmatic rocks. In classification of Neelov (1980), indications of this are the elevated K_2O but low MgO and CaO contents. Thus, provenances of metasediments from the Erzin Complex were of diverse lithology and characterized by recycling of formerly accumulated sediments.

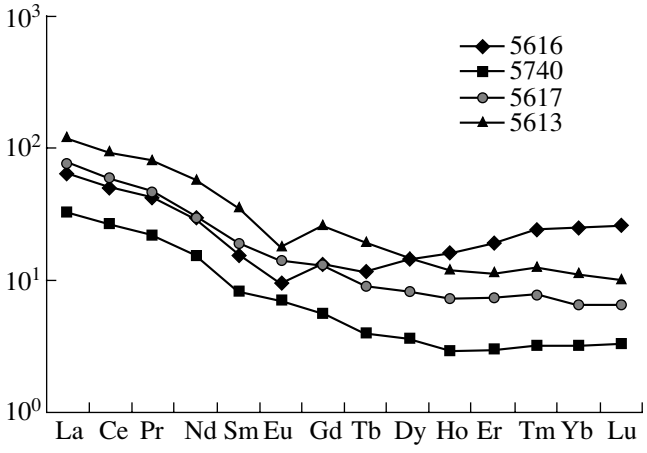

Fig. 3. Chondrite-normalized REE concentrations in metasediments of Tuva–Mongolian massif.

Normal and calcareous subarkosic sandstones were the respective protoliths for two-pyroxene (Sample 5617) and hypersthene (Sample 5546) gneisses of the Erzin Complex. The REE spectrum and indicative ratios $(La/Yb)_N$ = 11.9, La/Sc = 2.1, and Th/Sc = 0.61 in subarkosic sandstones are comparable with proper characteristics of rocks in ensialic volcanic arcs (Taylor and McLennan, 1995). In general, metasediments of the Erzin Complex were deposited in back-arc basins, where clastic sedimentation was dominated by erosion products of andesite–dacitic volcanics and complicated by subsequent redeposition of sediments in shallow shelf settings of marginal seas (McLennan *et al.*, 1993).

Naryn Complex. Two-mica quartzose schists (Sample 5740) from metasedimentary succession of the Naryn Complex are similar in composition to subarkosic sandstones. Typical of the schists are low REE concentrations, absence of Eu-anomaly (Eu/Eu* = 1.02, Table 2), high ratio $(La/Yb)_N$ = 9.9, and values La/Sc =2.5 and Th/Sc = 0.8. Geochemical parameters point to contribution of provenances composed of silicic and mafic rocks (Cullers, 2000) that is most characteristic of Phanerozoic sediments accumulated under influence of erosion of basalt–andesite–dacite volcanic series of ensialic island arcs or active continental margins (Taylor and McLennan, 1985). Biotite gneiss from an interlayer in carbonate succession of the Naryn Complex (Sample 5553) corresponds in composition to Mg–Na greywacke sandstone and implies that provenance of clastic material was composed predominantly of intermediate to basic rocks. Terrigenous metasediments of the complex characterize a fan of immature sediments in a past island-arc basin, where influence of continental provenances was less significant than during accumulation period of the Erzin and Moren complexes.

GEOCHRONOLOGICAL RESULTS

The results of U–Th–Pb geochronological investigation of zircons from terrigenous metasediments of the Moren and Erzin complexes are presented in Table 3 and interpreted in respective diagrams (Figs. 4 and 5). Sampling sites are shown in Fig. 2.

Table 3. Results of SHRIMP^{TM} zircon dating for metamorphic rocks of the Tuva–Mongolian massif

Analysis no.	Analyzed material	Concentration, ppm		Th/U	Isotopic ratios				Age, Ma			K, %
		U	Th		$^{206}Pb/^{204}Pb$	$^{207}Pb/^{206}Pb$	$^{207}Pb/^{235}U$	$^{206}Pb/^{238}U$	$^{206}Pb/^{238}U$	$^{207}Pb/^{235}U$	$^{207}Pb/^{206}Pb$	
Sample 5613, disthene–garnet–biotite gneiss, Moren Complex												
5613/1.1	Center of prismatic, weakly zoned crystal	222	265	1.20	209205	0.0650 ± 8	1.168 ± 49	0.1303 ± 51	789 ± 29	786 ± 23	776 ± 25	102
5613/2.1	Ditto	166	163	0.98	35587	0.0666 ± 10	1.202 ± 74	0.1309 ± 76	793 ± 43	802 ± 35	825 ± 33	96
5613/3.1	Ditto	51	46	0.90	1944	0.0607 ± 28	1.061 ± 62	0.1268 ± 38	770 ± 22	734 ± 31	628 ± 102	123
5613/4.1	Apex of short prismatic translucent unzoned crystal	628	646	1.03	6664	0.0631 ± 7	1.061 ± 53	0.1219 ± 57	742 ± 33	734 ± 26	711 ± 24	104
5613/5.1	Apex of short prismatic homogeneous broken crystal zoned weakly	145	90	0.62	4699	0.0641 ± 13	1.265 ± 41	0.1432 ± 33	863 ± 19	830 ± 18	743 ± 42	116
5613/6.1	Apex of short prismatic homogeneous crystal zoned weakly	98	53	0.54	4541	0.0622 ± 36	1.334 ± 74	0.1323 ± 30	801 ± 17	769 ± 36	680 ± 129	118
5613/7.1	Ditto	81	60	0.74	3138	0.0639 ± 33	1.098 ± 66	0.1245 ± 34	756 ± 19	752 ± 33	740 ± 111	102
5613/9.1	Center of prismatic translucent zoned crystal (core?)	173	156	0.90	6344	0.0656 ± 17	1.213 ± 50	0.1341 ± 43	811 ± 25	807 ± 25	793 ± 55	102
5613/10.1	Center of short prismatic translucent zoned crystal (partially recrystallized?)	93	69	0.74	7019	0.0673 ± 24	1.208 ± 57	0.1303 ± 36	789 ± 21	804 ± 27	846 ± 75	93
5613/11.1	Apex of prismatic translucent zoned crystal (partially recrystallized?)	137	101	0.73	7080	0.0641 ± 19	1.063 ± 43	0.1204 ± 28	733 ± 16	735 ± 21	744 ± 65	99
5613/12.1	Center of prismatic translucent zoned crystal	279	269	0.96	7501	0.0651 ± 9	1.038 ± 46	0.1157 ± 46	705 ± 27	723 ± 23	777 ± 31	91
5613/13.1	Center of short prismatic translucent homogeneous crystal (recrystallized?)	58	38	0.65	932	0.0599 ± 56	1.033 ± 107	0.1252 ± 43	760 ± 25	720 ± 55	598 ± 218	127
5613/14.1	Center of short prismatic translucent homogeneous crystal (recrystallized?)	181	155	0.86	8398	0.0640 ± 13	1.057 ± 54	0.1199 ± 54	730 ± 31	733 ± 27	741 ± 42	99
5613/15.1	Center of prismatic transparent homogeneous crystal	48	62	1.30	1948	0.0626 ± 42	1.092 ± 89	0.1265 ± 51	768 ± 29	750 ± 44	695 ± 148	111
5613/16.1	Center of prismatic transparent zoned crystal	171	179	1.05	7702	0.0656 ± 22	1.099 ± 61	0.1216 ± 48	740 ± 28	753 ± 30	793 ± 73	93
5613/17.1	Ditto	287	201	0.70	897	0.0558 ± 61	0.795 ± 94	0.1033 ± 36	634 ± 21	594 ± 54	444 ± 261	143

Table 3. (Contd.)

Analysis no.	Analyzed material	Concentration, ppm		Th/U	Isotopic ratios				Age, Ma			K, %
		U	Th		$^{206}Pb/^{204}Pb$	$^{207}Pb/^{206}Pb$	$^{207}Pb/^{235}U$	$^{206}Pb/^{238}U$	$^{206}Pb/^{238}U$	$^{207}Pb/^{235}U$	$^{207}Pb/^{206}Pb$	
5613/18.1	Center of prismatic crystal	415	218	0.53	11834	0.0945 ± 12	2.652 ± 70	0.2035 ± 44	1194 ± 24	1315 ± 20	1519 ± 24	79
5613/19.1	Center of short prismatic translucent zoned crystal (core?)	271	261	0.96	10320	0.0663 ± 8	1.207 ± 33	0.1321 ± 32	800 ± 18	804 ± 16	814 ± 24	98
5613/19.2	Marginal area of short prismatic translucent zoned crystal (homogeneous envelope?)	130	50	0.38	2414	0.0653 ± 27	1.112 ± 70	0.1236 ± 51	751 ± 29	759 ± 34	783 ± 91	96
5613/20.0	Center of prismatic translucent zoned crystal	229	186	0.81	6146	0.0652 ± 16	1.114 ± 48	0.1239 ± 41	753 ± 23	760 ± 23	782 ± 51	96
Sample 5616, spinel–sillimanite-cordierite gneiss, Erzin Complex												
5616/1.1	Core of prismatic translucent zoned crystal	397	245	0.62	2591	0.0699 ± 14	1.328 ± 49	0.1379 ± 38	833 ± 22	858 ± 21	924 ± 43	90
5616/2.1	Center of prismatic translucent zoned crystal	422	268	0.64	2094	0.0669 ± 24	1.180 ± 72	0.1278 ± 57	776 ± 33	791 ± 34	836 ± 78	93
5616/3.1	Core of short prismatic homogeneous crystal partially recrystallized	145	169	1.16	4382	0.1699 ± 34	10.52 ± 65	0.4491 ± 25	2391 ± 113	2482 ± 59	2557 ± 34	94
5616/4.1	Envelope of prismatic transparent zoned crystal	274	178	0.65	1040	0.0588 ± 30	0.619 ± 46	0.0764 ± 37	474 ± 22	489 ± 29	560 ± 114	85
5616/5.1	Core of prismatic translucent and fissured crystal	484	320	0.66	4250	0.0659 ± 15	0.986 ± 58	0.1086 ± 56	665 ± 32	697 ± 30	802 ± 48	83
5616/6.1	Center of short prismatic transparent zoned crystal (core?)	119	61	0.51	711	0.0656 ± 59	1.267 ± 136	0.1402 ± 68	846 ± 39	831 ± 63	792 ± 200	107
5616/7.1	Center of prismatic translucent crystal	629	186	0.30	2495	0.0628 ± 20	0.935 ± 49	0.1080 ± 40	661 ± 23	670 ± 26	703 ± 70	94
5616/8.1	Apex of prismatic transparent homogeneous crystal	124	44	0.36	1236	0.0692 ± 44	1.128 ± 103	0.1181 ± 68	720 ± 40	767 ± 50	905 ± 136	80
5616/9.1	Center of prismatic translucent zoned crystal	423	67	0.16	2966	0.0897 ± 13	1.553 ± 73	0.1256 ± 54	763 ± 31	952 ± 29	1419 ± 28	54
Sample 5617, two-pyroxene gneiss, Erzin Complex												
5617/1.1	Center of prismatic zoned crystal (core?)	124	118	0.95	1158	0.0629 ± 40	1.173 ± 94	0.1354 ± 57	818 ± 32	788 ± 45	704 ± 141	116
5617/2.1	Center of prismatic transparent zoned crystal	114	88	0.77	1010	0.0683 ± 47	1.124 ± 93	0.1194 ± 45	727 ± 26	765 ± 45	878 ± 149	83

Table 3. (Contd.)

Analysis no.	Analyzed material	Concentration, ppm		Th/U	Isotopic ratios				Age, Ma			K, %
		U	Th		$^{206}Pb/^{204}Pb$	$^{207}Pb/^{206}Pb$	$^{207}Pb/^{235}U$	$^{206}Pb/^{238}U$	$^{206}Pb/^{238}U$	$^{207}Pb/^{235}U$	$^{207}Pb/^{206}Pb$	
5617/3.1	Ditto	49	24	0.49	480	0.0747 ± 131	1.305 ± 303	0.1267 ± 168	769 ± 97	848 ± 143	1060 ± 400	73
5617/4.1	Center of prismatic transparent homogeneous crystal	119	76	0.64	1534	0.0766 ± 29	1.597 ± 100	0.1513 ± 68	908 ± 38	969 ± 40	1110 ± 78	82
5617/5.1	Center of prismatic transparent homogeneous crystal partially recrystallized	62	48	0.77	662	0.0812 ± 70	1.264 ± 150	0.1129 ± 81	690 ± 47	830 ± 70	1226 ± 179	56
5617/5.2	Marginal zone of prismatic transparent homogeneous crystal partially recrystallized	70	61	0.87	632	0.0781 ± 74	1.513 ± 166	0.1404 ± 65	847 ± 37	936 ± 70	1150 ± 199	74
5617/6.1	Center of prismatic translucent zoned crystal	106	49	0.46	727	0.0756 ± 93	1.278 ± 179	0.1226 ± 65	745 ± 37	836 ± 83	1085 ± 267	69
5617/7.1	Center of prismatic transparent zoned crystal	155	66	0.43	1526	0.0723 ± 39	1.421 ± 98	0.1426 ± 52	859 ± 30	898 ± 42	994 ± 113	87
5617/8.1	Ditto	95	39	0.41	707	0.0699 ± 49	1.322 ± 111	0.1371 ± 54	828 ± 31	855 ± 50	926 ± 149	89
5617/9.1	Center of isometric transparent non-luminescent crystal	859	361	0.42	6511	0.0680 ± 17	1.282 ± 62	0.1368 ± 54	826 ± 31	838 ± 28	867 ± 51	95
5617/10.1	Apex of prismatic crystal showing bright luminescence	36	20	0.56	257	0.0748 ± 139	0.917 ± 210	0.0890 ± 100	550 ± 59	661 ± 118	1062 ± 429	52
5617/11.1	Center of prismatic translucent zoned crystal	73	46	0.63	1597	0.0684 ± 80	1.220 ± 156	0.1294 ± 50	785 ± 29	810 ± 74	880 ± 264	89
5617/12.1	Center of prismatic translucent homogeneous crystal	154	71	0.46	2695	0.0691 ± 30	1.346 ± 101	0.1412 ± 79	851 ± 45	866 ± 45	902 ± 91	94
5617/13.1	Center of prismatic translucent zoned crystal	136	76	0.56	1020	0.0681 ± 37	1.249 ± 100	0.1330 ± 71	805 ± 40	823 ± 46	872 ± 115	92
5617/14.1	Center of transparent zoned fragment of prismatic crystal	178	60	0.34	1322	0.0618 ± 49	1.013 ± 100	0.1188 ± 59	724 ± 34	710 ± 52	668 ± 178	108
5617/14.2	Center of transparent zoned fragment of prismatic crystal	173	76	0.44	266	0.0841 ± 127	1.429 ± 244	0.1233 ± 78	749 ± 45	901 ± 108	1294 ± 326	58
5617/15.1	Center of prismatic translucent zoned crystal	193	28	0.15	1422	0.0689 ± 35	1.244 ± 78	0.1310 ± 40	794 ± 23	821 ± 36	896 ± 108	89
5617/16.1	Center of prismatic translucent zoned crystal	127	64	0.51	1360	0.0676 ± 30	1.349 ± 77	0.1447 ± 46	871 ± 26	867 ± 34	857 ± 95	102

Table 3. (Contd.)

Analysis no.	Analyzed material	Concentration, ppm		Th/U	Isotopic ratios				Age, Ma			K, %
		U	Th		$^{206}Pb/^{204}Pb$	$^{207}Pb/^{206}Pb$	$^{207}Pb/^{235}U$	$^{206}Pb/^{238}U$	$^{206}Pb/^{238}U$	$^{207}Pb/^{235}U$	$^{207}Pb/^{206}Pb$	
5617/17.1	Ditto	200	61	0.31	2100	0.0710 ± 20	1.264 ± 72	0.1292 ± 60	783 ± 34	830 ± 33	957 ± 59	82
5617/18.1	Center of translucent zoned fragment of prismatic crystal	91	100	1.10	455	0.0579 ± 102	1.092 ± 199	0.1368 ± 41	826 ± 23	750 ± 102	527 ± 442	157
5617/19.1	Center of isometric translucent zoned crystal	40	24	0.60	321	0.0663 ± 89	1.271 ± 219	0.1390 ± 126	839 ± 72	833 ± 103	816 ± 310	103
5617/20.1	Apex of prismatic translucent zoned crystal	91	52	0.57	459	0.0658 ± 99	1.200 ± 193	0.1324 ± 51	801 ± 29	801 ± 93	798 ± 354	100
5617/21.1	Core of prismatic translucent zoned crystal with a weak luminescence	219	95	0.43	4470	0.1186 ± 14	5.287 ± 185	0.3235 ± 102	1807 ± 50	1867 ± 30	1935 ± 21	93
5617/22.1	Center of translucent crystal fragment with a weak luminescence	167	108	0.65	1016	0.0695 ± 37	1.321 ± 95	0.1379 ± 58	833 ± 33	855 ± 42	912 ± 113	91
5617/24.1	Center of prismatic translucent zoned crystal	109	64	0.59	778	0.0831 ± 51	1.486 ± 114	0.1298 ± 51	787 ± 29	925 ± 48	1271 ± 123	62
5617/25.1	Center of prismatic translucent homogeneous crystal	85	58	0.68	561	0.0749 ± 87	1.433 ± 184	0.1388 ± 61	838 ± 34	903 ± 80	1066 ± 252	79
5617/26.1	Center of prismatic translucent zoned crystal	77	74	0.96	979	0.0867 ± 101	1.475 ± 187	0.1234 ± 47	750 ± 27	920 ± 80	1353 ± 242	55
5617/27.1	Envelope of isometric translucent homogeneous crystal	244	117	0.48	688	0.0689 ± 40	1.294 ± 114	0.1362 ± 82	823 ± 47	843 ± 52	895 ± 124	92
5617/28.1	Center of prismatic translucent zoned crystal (partially recrystallized)	148	1	0.01	827	0.0652 ± 38	1.236 ± 85	0.1376 ± 41	831 ± 23	817 ± 39	781 ± 126	106
5617/29.1	Apex of prismatic translucent crystal fragment with a weak luminescence	289	4	0.01	1967	0.0685 ± 17	1.364 ± 66	0.1444 ± 55	870 ± 31	874 ± 29	885 ± 52	98
5617/30.1	Center of prismatic translucent zoned crystal	237	252	1.06	2039	0.0660 ± 28	1.252 ± 125	0.1375 ± 118	831 ± 67	824 ± 58	807 ± 90	103
5617/31.1	Center of prismatic translucent zoned crystal	139	77	0.56	867	0.0658 ± 53	1.229 ± 119	0.1355 ± 59	819 ± 34	814 ± 56	799 ± 180	103

Note: K is concordance degree in %.

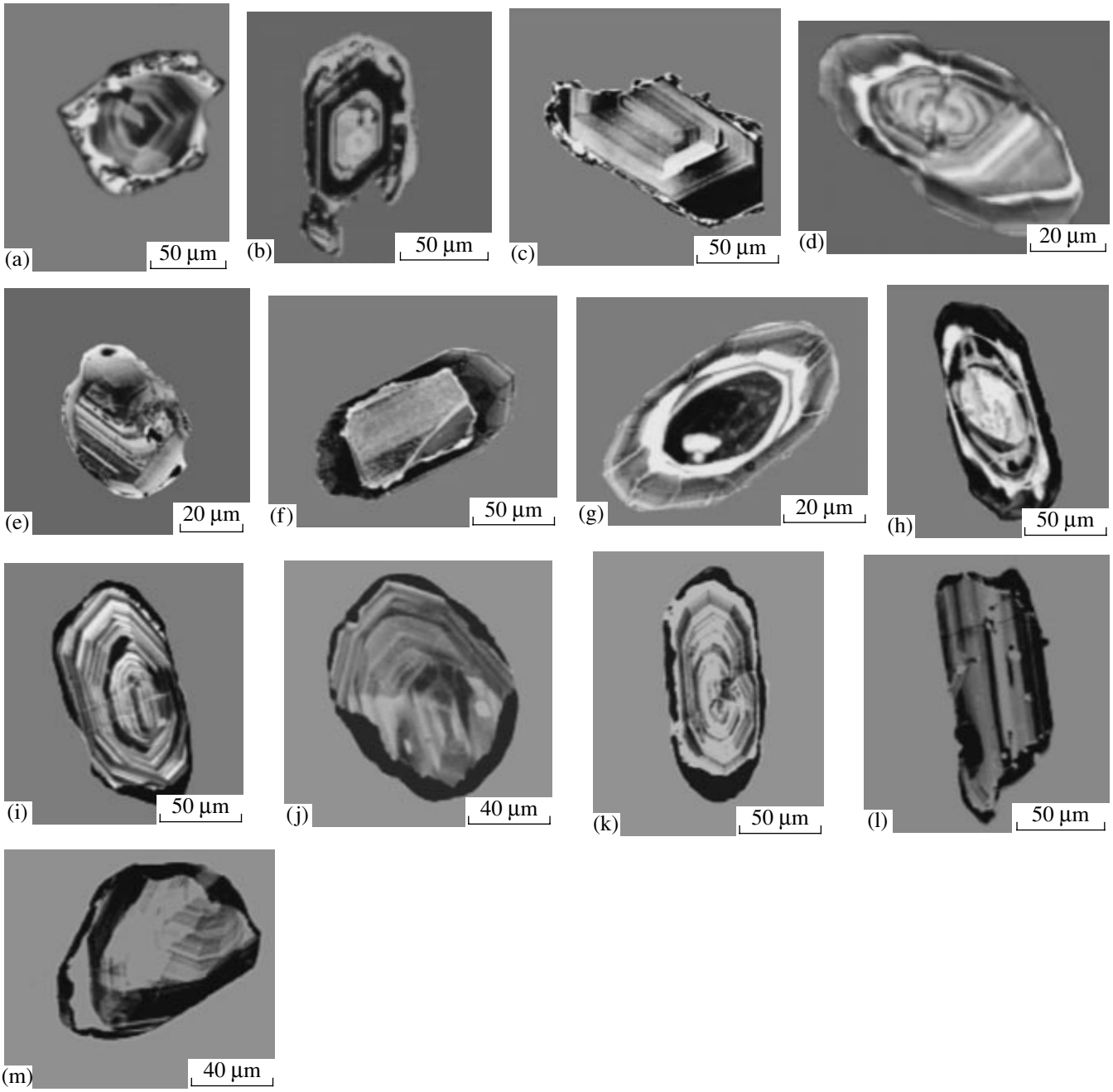

Fig. 4. Habits and internal structures of zircon crystals as seen via cathodoluminescence detector of scanning electron microscope CamScan (accelerating voltage 15 KV): (a, b, c) zircons from garnet–disthene–biotite gneiss, Moren Complex, Sample 5613; (d–h) zircons from spinel–cordierite–sillimanite gneiss, Erzin Complex, Sample 5616; (i–m) two-pyroxene gneiss, Erzin Complex, Sample 5617.

Garnet–disthene–biotite gneiss (polymictic sandstone), Moren Complex (Sample 5613). Accessory detrital zircon from the sample is represented by subidiomorphic transparent and semitransparent pinkish crystals of prismatic to short prismatic habit. Fine magmatic zoning is "truncated" in outer rims by unzoned domains with a bright luminescence (Figs. 4a and 4b), which were likely formed during recrystallization in the course of superimposed high-T metamorphism. In addition, some crystals have cores (Fig. 5b). Zircon grains range in size from 30 to 100 μm.

We analyzed 19 zircon grains. As one can see from Table 4 and Fig. 5a, ages estimated for the grains studied are mostly concordant (concordance degree 98 to 103%). The estimated age values range from 0.70 to 0.82 Ga. The average $^{206}Pb/^{238}U$ age calculated from 16 analytical results for central and marginal areas of

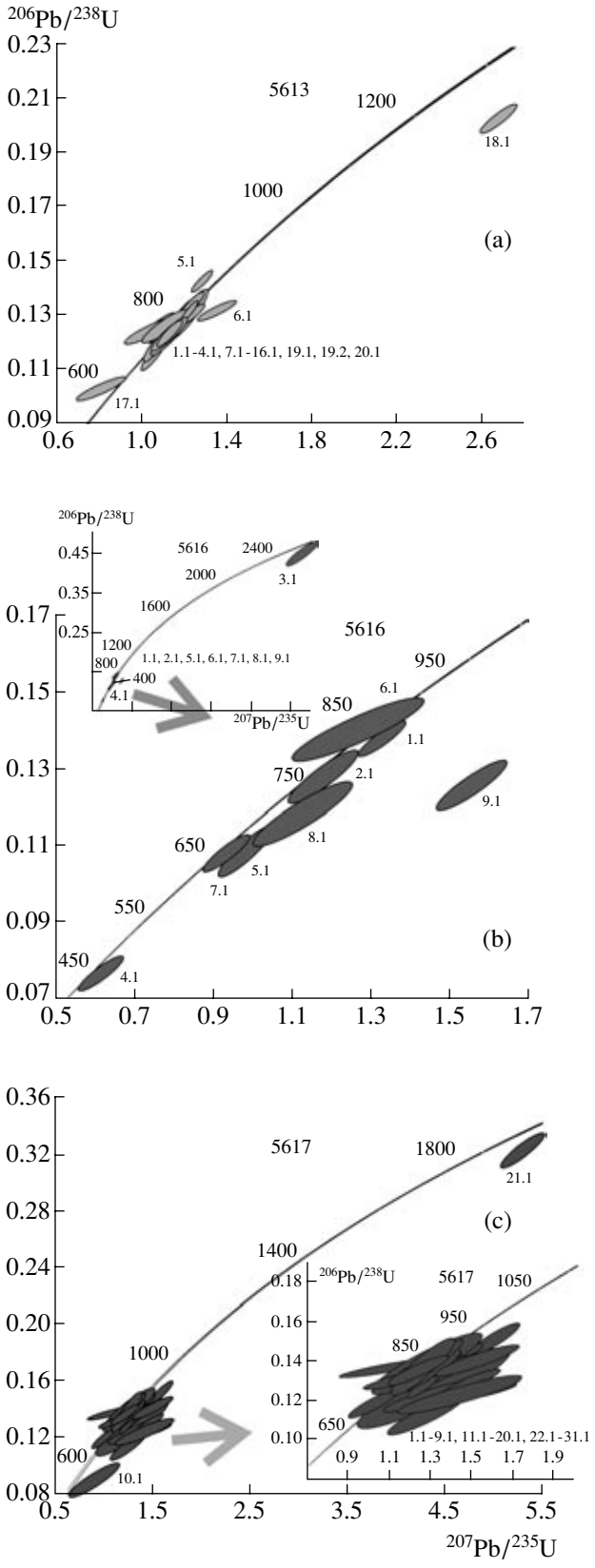

Fig. 5. Isotopic diagrams with results of U–Pb zircon dating obtained using ion microprobe SHRIMP^{TM} II: (a) sample 5613; (b) Sample 5616; (c) Sample 5617.

crystals is 767 ± 15 Ma (MSWD = 6.6). An older $^{207}Pb/^{206}Pb$ age of 1519 ± 24 Ma is obtained for a single prismatic crystal lacking core (no. 18.1 in Table 3).

Spinel–sillimanite–cordierite gneiss (shale), Erzin Complex (Sample 5616). Zircon crystals from Sample 5616 are transparent to semitransparent, colorless, subidiomorphic, prismatic to short prismatic and rounded in shape, showing a high birefringence. Characteristic of crystals are zoned, partially recrystallized cores (as is seen under cathodoluminescence: zoned areas are partially or completely replaced by homogeneous domains, while rims are usually unzoned (Figs. 4d to 4f). Crystals are not greater than 60 μm in size.

We analyzed isotopic composition of nine zircon crystals (Table 3, Fig. 5b). The oldest $^{207}Pb/^{206}Pb$ age of 2557 ± 34 Ma is obtained for the core of one crystal (no. 3.1 in Table 3), whereas the $^{206}Pb/^{238}U$ age of rim in other crystal (no. 4.1 in Table 3) is 474 ± 22 Ma. The last value is consistent with the date estimated for granulite metamorphism that affected the Erzin Complex (SHRIMP date of 494 ± 11 Ma, Sal'nikova *et al.*, 2001). The $^{206}Pb/^{238}U$ age assessments for other seven grains of zircon are within the interval of 661–846 Ma. We failed to figure out the precise age of this zircon generation because of limited number of measurement results.

Two-pyroxene gneiss (subarkosic sandstone), Erzin Complex (Sample 5617). Detrital zircon from Sample 5617 is represented by transparent to semitransparent, subidiomorphic, pale-yellow crystals prismatic to short prismatic and isometric in shape. Under cathodoluminescence, crystals show magmatic zoning and thin unzoned envelopes discordant relative to zoning (Figs. 4g and 4h). Crystals range in size from 30 to 150 μm.

Data points for majority of 30 analyzed crystals (Fig. 5c) plot close to concordia, and respective concordant ages (concordance degree 98–103%) are within the interval of 0.76–0.90 Ga. The average $^{206}Pb/^{238}U$ age calculated based on 29 age values for central and marginal zones of crystals is 809 ± 17 Ma (MSWD = 8.2). The core distinguished in one crystal yielded the much older $^{207}Pb/^{206}Pb$ age of 1935 ± 21 Ma (no. 21.1 in Table 3).

In conclusion, we would like to stress that many detrital zircons from metasediments of the Moren and Erzin complexes have a magmatic origin, and magmatic source rocks were therefore widespread in provenances of clastic material. Metamorphic overgrowthes and partial recrystallization in some zircon crystals from the Erzin Complex are products of the granulite-facies metamorphism that took place, as is established earlier (Sal'nikova *et al.*, 2001) 494 ± 11 Ma ago according to results obtained using the ion microprobe SHRIMP^{TM} or between 497 ± 4 and 521 ± 12 Ma according to the U–Pb zircon dating of syn- and post-metamorphic granitoid intrusions.

Table 4. Sm-Nd isotopic data on supracrustal rocks of the Tuva–Mongolian massif

No.	Sample no.	Age, Ma	Sm, ppm	Nd, ppm	$^{147}Sm/^{144}Nd$	$^{143}Nd/^{144}Nd$ ($\pm 2\sigma$)	$\varepsilon_{Nd}(0)$	$\varepsilon_{Nd}(T)$	$T_{Nd}(DM)$	$T_{Nd}(DM_{-2st})$**
Moren Complex										
1	5613*	500	7.56	35.1	0.1305	0.512291 ± 9	–6.8	–2.5	1574	1454
2	5741	500	4.36	25.6	0.1032	0.511742 ± 5	–17.5	–11.5	1939	2196
3	5558-1	500	6.36	37.8	0.1017	0.511794 ± 10	–16.5	–10.4	1844	2104
Erzin Complex										
4	5616*	500	3.69	19.36	0.1157	0.511984 ± 11	–12.8	–7.6	1812	1872
5	5617*	500	3.78	19.94	0.1151	0.511981 ± 10	–12.8	–7.6	1806	1874
6	5525	500	6.99	37.0	0.1143	0.512133 ± 8	–9.9	–4.6	1560	1624
7	5546	500	5.50	26.6	0.1248	0.512114 ± 8	–10.2	–5.6	1775	1710
Naryn Complex										
8	5740	500	1.73	8.94	0.1174	0.511987 ± 11	–12.7	–7.6	1839	1876
9	5553	500	4.59	29.5	0.0940	0.512199 ± 9	–8.6	–2.0	1212	1410

Note: Rock types as in Table 1; samples subjected to U–Pb zircon dating are marked by asterisk; $T_{Nd}(DM)_{2st}$ is model age of regional metamorphism.

Nd ISOTOPIC SYSTEMATICS

Data of Sm–Nd isotopic analysis of metamorphic rocks from the Moren, Erzin, and Naryn complexes are presented in Table 4.

For *garnet–disthene–biotite gneiss* (polymictic sandstone) of the Moren Complex (Sample 5613), we calculated the Early Riphean values of $T_{Nd}(DM)$ = 1.6 Ga, $T_{Nd}(DM\text{-}2st)$ = 1.4 Ga, and parameter $\varepsilon_{Nd}(0.5)$ = –2.5. The older Early Proterozoic values $T_{Nd}(DM)$ = 1.8–1.9 Ga, $T_{Nd}(DM\text{-}2st)$ = 2.1–2.2 Ga, and $\varepsilon_{Nd}(0.5)$ = –11.5 and –10.4 are estimated for biotite gneisses of this complex (polymictic and subgraywacke sandstones).

Spinel–sillimanite–cordierite and two-pyroxene gneisses of the Erzin Complex (shales and sandstones) are characterized by Early Proterozoic $T_{Nd}(DM)$ = 1.6 Ga, $T_{Nd}(DM\text{-}2st)$ = 1.4 Ga, and by $\varepsilon_{Nd}(0.5)$ ranging from –4.6 to –7.6.

The *Nd model age of two-mica quartzose schist* (subacrosic sandstone) from terrigenous succession of the Naryn Complex is 1.8 Ga $\varepsilon_{Nd}(0.5)$ = –7.6, whereas $T_{Nd}(DM)$ = 1.2 Ga, $T_{Nd}(DM\text{-}2st)$ = 1.4 Ga, and $\varepsilon_{Nd}(0.5)$ = –2.0 are calculated for biotite gneiss from carbonate succession of the complex.

DISCUSSION

Concordant and subconcordant age values obtained for clastic zircons from metasedimentary rocks of the Moren and Erzin complexes are mostly within two geochronological intervals of 0.70–0.82 and 0.76–0.90 Ga respectively. In other words, the rock successions under consideration are not older than 0.70–0.76 Ga. Their upper age limit is evident from the U–Pb age of 536 ± 6 Ma obtained for crosscutting granitoids (Kozakov *et al.*, 1999; Sal'nikova *et al.*, 2001) that corresponds approximately to the Vendian–Cambrian boundary (Semikhatov, 2000). Thus, it is possible to suggest that terrigenous protoliths of the Moren and Erzin complexes accumulated during the terminal Late Riphean–Vendian.

The associated problem of possible basement and provenances can be solved based on Nd isotopic data. Discussing the problem, we should bear in mind that Nd model ages, being dependent on mixing processes, not always correspond to the crust formation time. To prove the crust-forming stages of respective ages we should have rocks with $\varepsilon_{Nd}(T)$ values close to those in depleted mantle (DePaolo, 1981; Patchett, 1992).

The Nd model ages estimated for metasedimentary rocks of the Moren, Erzin, and Naryn complexes are much greater (1.6–2.1 Ga) than the age of sedimentation. They are close to Nd model ages of granitoids present in the Early Baikalian volcano-plutonic associations (0.75–0.9 Ga old) fringing the Siberian platform. For instance, Vernikovskaya *et al.* (2002) reported the Nd model ages of 1.5 to 1.6 and 1.8 to 2.0 Ga granitoids of the Mamontovo–Shrenkovo terrane in the central Taimyr, which are 880–940 Ma old (U–Pb zircon dating). According to petrochemical data, the granitoid magmatism in the Taimyr fold system was connected with magma generation from mantle and crust–mantle sources (Vernikovskii *et al.*, 1999). The Nd model ages of 1.9–2.1 Ga calculated for crustal post-collision granitoids of the Yenisei Range, which are 720–760 Ma old according to U–Pb ages of zircon and monazite, also characterize the mixing events but not the crust-forming processes of that time (Vernikovskii *et al.*, 2002). The Early–Middle Riphean values of Nd model ages characterize granitoids of microcontinents in Central Asia ("Precambrian isotopic province" after Kovalenko *et al.*,

1996, 1999), where they also depict mixing processes (Kozakov *et al.*, 2003, 2004). Indications of Early–Middle Riphean crust-forming processes have not been detected as well in the Central Asian foldbelt (Kovalenko *et al.*, 1996, 1999; Yarmolyuk *et al.*, 1999).

The Early–Middle Riphean Nd model ages are similarly untypical of crystalline rocks from the basement of Siberian platform (Kovach *et al.*, 2000). For the Early Proterozoic post-collision granitoids of the Sharyzhalgai block in the Sayan marginal ledge that is directly connected with structures of Central Asian foldbelt, the Nd model ages are calculated within the interval of 3.0–2.8 Ga, and the Nd model ages of 3.3–2.9 Ga are determined for gneissic rocks of the Sharyzhalgay Complex enclosing the above granitoids. The Early Proterozoic granitoids of the Biryusa block and Angara–Kan ledge are characterized by 2.4–2.7 Ga Nd model ages and their country gneisses of the Kuzeev complex (Angara–Kan ledge) have Nd model age of 2.6–2.7 Ga (Kirnozova *et al.*, 2003). The oldest value of Nd model ages (3.48 Ga) is established in the Onot greenstone belt for tonalite–trondhjemite association with zircons that are 3287 ± 8 Ma old (Bibikova *et al.*, 2002). The interval of Nd model ages calculated for Archean rocks of the Dzabkhan microcontinent is 3.0–3.3 Ga (Kozakov *et al.*, 1997). It is clear therefore that crystalline rocks of ancient cratons or their fragments were not the only source for the studied rocks from the Late Riphean volcano-plutonic associations.

Thus, the Nd isotopic systematics, geochemical indicators, and data on origin and ages of zircons from metasediments of the Moren and Erzin complexes suggest that the calculated Nd model ages (1.5–2.0 Ga) are indicative of the clastic material origin from different source rocks and do not correspond to real stages of crust formation. Let us consider the problem of possible source rocks.

As one can judge from geochronological, geochemical and isotopic data, there were basic, intermediate, and silicic rocks of Late Riphean ensialic island arcs in provenances of metasediments of the Moren and Erzin complexes. Fragments of these structures are distinguished now as fringing the Siberian platform from the north, west, and south (Kuzmichev *et al.*, 2000a; Rytsk *et al.*, 2001; Vernikovskii *et al.*, 1999, 2001; Vernikovskaya *et al.*, 2002a, 2002b; Khain *et al.*, 2002). At first sight, volcanic arcs of that age could be formed along periphery of Siberian craton (Kuzmichev *et al.*, 2001; Dobretsov *et al.*, 2003; Kuzmichev, 2004). However, any signs of Late Riphean and Caledonian accretion or collision processes are unknown in marginal ledges of the platform basement along the distance of about 2500 km. In contrast, they are well manifested in fringing foldbelts directly at the contact with basement ledges as metamorphic events, folding of the platform cover, and magmatic activity of that age (Kozakov *et al.*, 2002; Yarmolyuk *et al.*, 2003). Within the Siberian platform, sediments of the time span 1000–850 Ma are represented mainly by shallow-shelf siliciclastic–carbonate deposits of epicontinental basins and aulacogens, being of reduced thickness or absent in many areas (Semikhatov and Serebryakov, 1983; Rainbird *et al.*, 1998; Semikhatov *et al.*, 2002). Their chemical composition suggests erosion of pre-Riphean basement rocks of the platform and insignificant contribution of the Late Riphean juvenile substance from a "non-Siberian source" that was outside the craton (Podkovyrov *et al.*, 2001). As is assumed, structures of the Central Asian foldbelt were separated from Siberian craton by an oceanic basin (Zonenshain *et al.*, 1990). It is difficult so far to figure out the time, when the Caledonian superterrane and Siberian craton became amalgamated into a single continent, although this tectonic event likely culminated before the Devonian (Zonenshain *et al.*, 1990), because since that time a common style of tectonic deformations is recoded in the platform and foldbelt. It is believed that two megastructures became conjoint along a large shear zone resembling transform fault (Rozen and Fedorovskii, 2001; Yarmolyuk *et al.*, 2003). It is also remarkable that the Siberian, North and South China blocks were presumably spaced closely within the Rodinia during the Late Riphean 800–780 Ma ago (Zhai *et al.*, 2003). Granitoids about 800 Ma old are known in the Yangtze block (Kröner *et al.*, 1993; Xue *et al.*, 1996). Fragmented ophiolites as old as 0.88–0.75 Ga are situated along the northern margin of the North China platform (Mossakovskii *et al.*, 1993). Granitoids 916 ± 16 Ma old are established in the metamorphic complex of the South Gobi microcontinent (Wang *et al.*, 2001). All together, these rock associations could represent the source of clastic material for metasediments of the Tuva–Mongolian massif, although it is impossible so far to determine the original tectonic position of above structural–lithologic complexes.

Older continental rocks (or products of their destruction) presumably also existed in provenances, as it follows from the Early Riphean (1.52 Ga) and pre-Riphean (1.94 and 2.56 Ga) ages determined for detrital zircons. These dates characterize most likely the provenances of Late Riphean structural–lithologic complexes, which turned into source of protoliths for the Late Riphean–Vendian metasediments of the Tuva-Mongolian massif. Influx of "ancient" material into sedimentary basins was likely controlled by erosion of Early Precambrian crystalline rocks in cratons and microcontinents with the pre-Riphean basement, e.g., in the Dzabkhan microcontinent (Fig. 1).

The known models of geodynamic evolution of the Central Asian foldbelt are controversial. Some researchers suggested that structures of the belt originated in the course of a long (over 800 m.y.) tectonic development of Paleo-Asian ocean since the terminal Middle or initial Late Riphean till the Carboniferous (Mossakovskii *et al.*, 1993; Didenko *et al.*, 1994). It was also suggested that folded accretionary structures, microcontinents of the Gondwanan group included,

drifted across a considerable distance from eastern Gondwana toward Siberian continent. The Dzabkhan, Tuva–Mongolian, and South Gobi microcontinents were among them. In opinion of other geologists (Berzin *et al.*, 1994; Belichenko and Boos, 1988), the Tuva–Mongolian massif and Dzabkhan microcontinent belonged to the Laurasian group and represented during the Riphean one continental mass, a part of Siberian craton. The model by Sengör *et al.* (1994) speculates on accretion of island-arc structures to a hypothetical volcanic arc during the formation of Central Asian foldbelt. Crystalline rock masses of a high metamorphic grade (those of the Tuva–Mongolian massif included), which occur northward of the Tarim and North China platforms, were attributed to the Late Precambrian basement of Eurosiberia and thus regarded as rafts of Siberian platform. In some other models, tectonic evolution of Paleo-Asian ocean was connected with the Rodinia breakup in the terminal Late Riphean (~730 Ma ago) under influence of the South Pacific superplume (Maruyama, 1994; Yarmolyuk and Kovalenko, 2001), and microcontinents were regarded as fragments of Rodinia shelf (Kovalenko *et al.*, 1999). As was suggested, the main phase of breakup and maximum opening of the Paleo-Asian ocean were in the terminal Late Riphean (Yarmolyuk and Kovalenko, 2002; Kovalenko *et al.*, 2003). The models argued for a juvenile origin of continental crust in Central Asia and for the crust formation due to accretion of Vendian–Cambrian island arcs, marginal basins, and fragments of Rodinia shelf with embedded oceanic islands. Dobretsov *et al.* (2003) considered the accretion and collision of above structures as progressing directly around Siberian craton in response to Rodinia breakup about 950 Ma ago in the initial Late Riphean. The Tuva–Mongolian massif was regarded therewith as a fragment of Siberian craton (Dobretsov, 2003).

Discussing geological history of Tuva–Mongolian massif in connection with general geodynamic constraints of the Early Caledonian accretion in Central Asia, we should bear in mind the following.

1. Petrochemical and geochemical data show that metasediments of the Moren, Erzin, and Naryn complexes accumulated in settings of a passive continental margin.

2. Provenances of clastic material hosted therewith the Late Riphean basic, intermediate, and silicic rocks.

3. Source rocks for metasediments of the massif belonged to the Early Baikalian volcano-plutonic associations.

4. In the accretionary collage of Central Asia, Archean basement is established in the Dzabkhan microcontinent and Gargan block, and only these structures can be regarded as fragments of ancient craton (Kozakov *et al.*, 1997a).

5. Geochemical data and Nd isotopic systematics for crustal granitoid intrusions of the Tuva–Mongolian massif imply that granitoid magmas originated in tectonic domains lacking pre-Riphean rocks and composed of the Late Riphean crust of transitional type (Yarmolyuk *et al.*, 1999; Kozakov *et al.*, 2003).

6. Geodynamic setting of that crust formation (a system of island arcs, back-arc basins, and passive margins) resembled situation that exited in southwestern Pacific during the Mesozoic and Cenozoic. It should be stressed therewith that total area of basins, where the crust of transitional type developed during c.a. 200 m.y., was comparable with area of ancient cratons (Zonenshain and Kuzmin, 1993).

To create a model of the Tuva-Mongolian massif formation in accretionary collage of Central Asia, it is necessary to presume first the Siberian craton position in supercontinent Rodinia and breakup time of the latter concurrent to opening of Paleo-Asian ocean. As premises can be different, alternative solutions of the problem are unavoidable. Nevertheless, we tried, using new data, to create a model as far self-consistent as possible, because the Tuva–Mongolian massif cannot be regarded at present as a fragment of Gondwana or Laurasia.

In our model, we presume that Siberia conjoint with Laurentia and Yangtze block was a part of supercontinent Rodinia (Hoffman, 1991; Rogers, 1996; Condie, 2001; Roger and Santosh, 2003; Zhai *et al.*, 2003). As is better evidenced, the southern (present-day coordinates) margin of Siberia was in contact with arctic margin of Laurentia (Rainbird *et al.*, 1998; Gallete *et al.*, 2000; Yarmolyuk and Kovalenko, 2001; Condie, 2002). It is likely as well that this situation retained till the end of the Early Proterozoic, when Siberian craton became a part of supercontinent Columbia (Rogers and Santosh, 2002). Rifting events that caused breakup of supercontinent Columbia took place 1.4 Ga ago (Condie, 2002), but Siberia and Laurentia existed in agglomerated state till the breakup of Rodinia (Didenko *et al.*, 2003). Admitting influence of the South Pacific superplume on lithosphere of Rodinia (Maruyama, 1994) and analyzing history of intraplate magmatism in Central Asia (Yarmolyuk and Kovalenko, 2001, 2003), we may assume that trans-lithospheric fracture responsible for separation of Siberia from Laurentia appeared in the terminal Late Riphean and developed from 720 to 650 Ma. In such a case, the initial stage of metasediments accumulation in the Tuva-Mongolian block is correlative to first approximation with the breakup of Rodinia. Volcano-plutonic associations, which were formed before or at the incipient stage of Rodinia breakup, represented likely the main source of clastic material. In other words, these volcano-plutonic associations originated and developed 1000–650 Ma ago in the Panthalassa that surrounded Rodinia, but not inside the craton between Siberia and Laurentia at the opening stage of Paleo-Asian ocean (Yarmolyuk and Kovalenko, 2003; Kozakov *et al.*, 2004). This conclusion does not exclude development of rifting events in and between continen-

tal blocks of Rodinia during the Late Riphean. In particular, the U–Pb zircon dating of anorogenic complexes showed that rifting events in the Yangtze block developed in two periods 830–795 and 780–745 Ma ago (Li *et al.*, 2003). Separation of East and West Gondwanan blocks and Laurentia was connected with the later period (about 750 Ma ago).

Based on data obtained in this and earlier works, the following scenario of the Tuva–Mongolian massif development can be suggested. About 1.0–0.73 Ga ago, rifting in marginal areas led to separation of fragments (microcontinents with pre-Riphean basement) from Rodinia, while volcanic arc, islands, back-arc and inter-arc basins formed in oceanic areas around the supercontinent (Yarmolyuk and Kovalenko, 2003). Events of accretion and collision are inferable from the Late Riphean manifestations of collision magmatism in fringing structures around Siberian platform, which took place 0.94–0.88 (Vernikovskaya *et al.*, 2002a, 2002b) or 0.8 Ga ago (Kuzmichev *et al.*, 2000) and were in progress until the opening of Paleo-Asian ocean 0.76–0.72 Ga ago (Vernikovskii, 2002a). Rocks formed during this period, products of their destruction, and Early Precambrian complexes of cratons and microcontinents formed provenances and basement for metasediments of the Tuva–Mongolian massif at the end of the Late Riphean–Vendian time (Kozakov *et al.*, 2003). If in the early Late Riphean (prior to Rodinia breakup) the East Gondwanan blocks were situated close to junction zone of Siberia and Laurentia (Hoffman, 1991; Dalziel, 1997; Condie, 2002; Li *et al.*, 2003; Zhai *et al.*, 2003), we may assume that the fringing volcano-plutonic association (in parts or completely) and cratonic fragments (Dzabkhan microcontinent and possibly Gargan block) drifted together with blocks of East Gondwana, the North to South China and Tarim blocks inclusive, during the Rodinia breakup and subsequent formation of Pangea (Mossakovskii *et al.*, 1993; Didenko *et al.*, 1994, 1999; Kheraskova *et al.*, 2003). As a result, the East Gondwanan blocks and transition zone that included extinct island arcs of the Late Riphean and cratonic fragments (Baidarik block) turned out to be opposite the Siberian craton. About 600 Ma ago, tectonic units split off that zone began to drift toward Siberia. In the course of several drift stages, they formed the Early Caledonian composite continent (superterrane) of Central Asia (Kozakov *et al.*, 2001), which incorporated remnants of Late Riphean volcanic arcs with carbonate platforms, microcontinents with pre-Riphean basement, Vendian ensimatic island arcs, oceanic islands and plateaus (Kozakov *et al.*, 2003; Yarmolyuk and Kovalenko, 2003). Erosion in provenances predominantly composed of the Late Riphean volcano-plutonic associations resulted in deposition of terrigenous sediments subsequently transformed into metamorphic rocks of the Moren, Erzin, and Naryn complexes. In the terminal Vendian (530–540 Ma ago), amalgamation of tectonic fragments was accompanied by low-grade metamorphism that affected the Moren Complex for instance (Kozakov *et al.*, 2001). The Early Caledonian accretionary collage was formed as a whole in the Late Cambrian after closure of short-lived Vendian oceanic basins (Didenko *et al.*, 1994; Ruzhentsev and Burashnikov, 1995). By the commencement of Ordovician, deep-seated rocks of Central Asian accretion zone were involved into a high-grade metamorphism (Kozakov, 2002).

Admitting opening of Paleo-Asian ocean in the initial Late Riphean about 1000–970 Ma ago (Khain *et al.*, 2002; Fedotova and Khain, 2002; Dobretsov, 2003; Dobretsov *et al.*, 2003), we should expect that development areas of Early Baikalian volcanic arcs were considerably spaced from Siberian craton. As was already mentioned, the Late Riphean events of accretion and collision, the earliest of which took place 940–880 Ma ago (Vernikovskaya *et al.*, 2002), left no records in marginal blocks and sedimentary cover of Siberian platform. Considering this, we should conclude that volcano-plutonic associations of the Late Riphean lower half or parts of them were formed most likely in Panthalassa. In the Paleo-Asian ocean properly, development of volcanic arcs and islands commenced probably in the terminal Late Riphean (Yarmolyuk and Kovalenko, 2003; Kheraskova *et al.*, 2003).

CONCLUSION

Geochronological results obtained in this work show that metasediments of the Moren and Erzin complexes of the Tuva-Mongolian massif were deposited in the terminal Late Riphean–Vendian in response to erosion in provenances predominantly composed of the Late Riphean rocks. The Nd isotopic systematics for granitoids and metamorphic rocks of the massif and for the Early Baikalian collision-accretionary complexes around Siberian platform suggest development of the Late Riphean crust-forming processes. Intensity of the latter is problematic, because respective rock complexes of that age are fragmentary preserved in fold structures of Central Asia. The Nd model ages calculated for granitoids of Caledonides and Hercynides mostly correspond to the Late Riphean (Kovalenko *et al.*, 1996). Accordingly, we may assume that development of volcanic arcs, islands, back-arc and inter-arc basins during the Late Riphean antedated the Rodinia breakup and lasted until opening of the Paleo-Asian ocean. The corresponding influx of juvenile material during 300–350 m.y. formed crust of the transitional type. That crust and products of its disintegration are now incorporated into basement of microcontinents and could be amalgamated with the Vendian–Early Paleozoic juvenile crust under Caledonides and Hercynides (Kozakov *et al.*, 2004). Data on secular variations in rates of juvenile crust generation (Condie, 2001) show a distinct minimum in the Middle Riphean (ca 1.35–0.95 Ga ago), the rate increase in the Late Riphean (ca 0.95–0.7 Ga ago), and a statistic maximum beginning since the Vendian.

The established secular variations of $^{87}Sr/^{86}Sr$ ratio in seawater imply that it was persistently low in the Grenvillian and post-Grenvillian oceans (Semikhatov *et al.*, 2002). Being as low as 0.70519–0.70566 during the early Late Riphean (1030–810 Ma), that ratio fluctuated from 0.70538 to 0.70686 775–690 Ma ago, became lower 660–640 Ma ago (0.70538–0.70580) and then increased up to 0.70840–0.70860 in the Vendian and Early Cambrian seawater (Kuznetsov *et al.*, 2003). The $^{87}Sr/^{86}Sr$ ratio decrease in seawater is dependent on a series of factors, the principal of which were likely the erosion of pre-Grenvillian mantle material in Grenvillides and/or a considerable influx of juvenile mantle components in the Late Riphean oceans. The low level of $^{87}Sr/^{86}Sr$ ratio in the Late Riphean seawater implies prevalence of mantle Sr influx over the continental one during the period of c.a. 200 m.y. (Kuznetsov *et al.*, 2003). It is possible therefore to connect the vast transgression of the initial Late Riphean (1030–810 Ma) with a high activity of mid-ocean ridges, and the combined influence of both factors lowered the $^{87}Sr/^{86}Sr$ ratio in seawater of that time (Semikhatov *et al.*, 2002; Kuznetsov *et al.*, 2003). The elevated spreading activity should be compensated by development of subduction zones. Nevertheless, admitting the commencement of Rodinia breakup in the terminal Late Riphean (Kovalenko *et al.*, 1999; Yarmolyuk and Kovalenko, 2001), we think that the Late Riphean volcanic arcs did not originate in the Paleo-Asian ocean (Fedotova and Khain, 2002). In our opinion, crust-forming processes and related origin of the Early Caledonian accretionary collage in Central Asia were connected first with the tectonic evolution of Panthalassa (initial half of the Late Riphean) and afterward with the development of Paleo-Asian ocean.

ACKNOWLEDGMENTS

We are grateful to M.A. Semikhatov for his valuable comments to our work. The work was supported by the Russian Foundation for Basic Research, project nos. 02-05-64208, 02-05-64196, 00-05-72011, by the Priority Program of Presidium RAS "Origin and Evolution of Biosphere," by program nos. 7 and 8 of the Earth Science Division RAS, and by the Foundation for Home Science Stimulation.

Reviewers V.V. Yarmolyuk and M.A. Semikhatov

REFERENCES

1. G. P. Aleksandrov, "Stratigraphy of Proterozoic and Lower Cambrian Deposits in Sangilen," in *Data on Geology of the Tuvinskaya ASSR* (Tuv. Kn. Izd., Kyzyl, 1991), pp. 39–57 [in Russian].
2. V. G. Belichenko and R. G. Boos, "The Bokson–Khubsugul–Dzabkhan Microcontinent in Paleozoic Structure of Central Asia," Geol. Geofiz., No. 12, 20–28 (1988).
3. V. G. Belichenko, E. F. Letnikova, and N. K. Geletii, "Geochemical Features of Carbonate Deposits in Covers of the Tuva-Mongolia Microcontinent," Dokl. Akad. Nauk **364** (1), 80–83 (1999) [Dokl. Earth Science **364** (1), 1–4 (1999)].
4. N. A. Berzin, R. G. Colman, N. L. Dobretsov, *et al.*, "Geodynamic Map of the Western Paleo-Asian Ocean," Geol. Geofiz. **35** (7–8), 8–28 (1994).
5. E. V. Bibikova, V. I. Levitskii, L. Z. Reznitskii, *et al.*, "Archean Tonalite–Trondhjemite Association in the Sayan basement Ledge of the Siberian Platform: U–Pb, Sm–Nd and Sr Isotopic Data," in *Proceedings of the All-Russia Scientific Conference "Geology, Geochemistry, and Geophysics at the Turning from XX to XXI Century* (Inst. Zemnoi Kory, Irkutsk, 2002), pp. 175–176 [in Russian].
6. J. C. Claoué-Long, W. Compston, J. Roberts, and C. M. Fanning, "Two Carboniferous Ages: A Comparison of SHRIMP Zircon Dating with Conventional Zircon Ages and $^{40}Ar/^{39}Ar$ Analysis," Spec. Publ. Soc. Sediment. Geol. **54**, 3–21 (1995).
7. W. Compston, I. S. Williams, and C. Myer, "U–Pb Geochronology of Zircons from Lunar Breccia 73217 Using a Sensitive High Mass-Resolution Ion Microprobe," J. Geophys. Res. **89B**, 525–534 (1984).
8. K. C. Condie, "Continental Growth During Formation of Rodinia," Gondwana Res. **4** (1), 5–16 (2001).
9. K. C. Condie, "Breakup of a Paleoproterozoic Supercontinent," Gondwana Res. **5** (1), 41–43 (2002).
10. R. L. Cullers, "The Geochemistry of Shales, Siltstones, and Sandstones of Pennsylvanian-Permian Age, Colorado, USA: Implications for Provenance and Metamorphic Studies," Lithos **51**, 181–203 (2000).
11. G. L. Cumming and J. R. Richard, "Ore Lead Isotope Ratios in a Continuously Changing Earth," Earth Planet. Sci. Lett. **28**, 155–171 (1975).
12. I. W. D. Dalziel, "Neoproterozoic–Paleozoic Geography and Tectonics: Review, Hypothesis Environmental Speculation," Bull. Geol. Soc. Am. **109**, 16–47 (1997).
13. D. J. DePaolo, "A Neodymium and Strontium Isotopic Study of Mesozoic Calk-Alkaline Granitic Batholiths of the Sierra Nevada and Peninsular Ranges, California," J. Geophys. Res. **86** (B11), 10470–10488 (1981).
14. A. N. Didenko, I. K. Kozakov, and V. Bakhtadze, "Paleomagnetism of the Early Proterozoic, the Baidarik Block of Central Mongolia," in *Proceedings of the Conference on Geological Evolution of Proterozoic Peri-Cratonic and Oceanic Structures in Northern Eurasia* (Tema, St. Petersburg, 1999), pp. 31–35 [in Russian].
15. A. N. Didenko, I. K. Kozakov, E. V. Bibikova, *et al.*, "Paleoproterozoic Granites of the Sharyzhalgai Block, Siberian Craton: Paleomagnetism and Geodynamic Inferences," Dokl. Akad. Nauk **390**, 368–373 (2003) [Dokl. Earth Science **390**, 510–515 (2003)].
16. A. N. Didenko, A. A. Mossakovskii, D. M. Pecherskii, *et al.*, "Geodynamics of Paleozoic Oceans in Central Asia," Geol. Geofiz. **35** (7–8), 59–75 (1994).
17. N. L. Dobretsov, "Structural Evolution of the Urals, Kazakhstan, Tien Shan, and Altai–Sayan Region in the Urals–Mongolian Foldbelt (Paleo-Asian Ocean)," Geol. Geofiz. **44** (1–2), 5–27 (2003).

18. N. L. Dobretsov, M. M. Buslov, and V. A. Vernikovsky, "Neoproterozoic to Early Ordovician Evolution of the Paleo-Asian Ocean: Implication to the Break-Up of Rodinia," Gondwana Res. **6** (2), 143–156 (2003).
19. V. F. Fedorovskii, A. G. Vladimirov, E. V. Khain, *et al.*, "Tectonics, Metamorphism, and Magmatism of Caledonian Collision Zones," Geotektonika, No. 3, 3–22 (1995).
20. A. A. Fedotova and E. V. Khain, *Tectonics of the Southern East Sayan Mountains and Their Position in the Urals–Mongolian Foldbelt* (Nauchnyi Mir, Moscow, 2002) [in Russian].
21. Y. Gallete, V. E. Pavlov, M. A. Semikhatov, and P. Yu. Petrov, "Late Mesoproterozoic Magnetostratigraphic Results from Siberia: Paleogeographic Implications and Magnetic Field Behavior," J. Geogr. Res. **105** (B7), 16481–16499 (2000).
22. A. S. Gibsher, A. A. Terleev, I. I. Vologdin, and A. M. Sugorakova, "The Composite Section of the Upper Precambrian Siliciclastic–Carbonate Complex in the Western Sangilen (SE Tuva)," in *The Late Precambrian and Early Paleozoic of Siberia, the Siberian Platform and Fringing Foldbelts* (Inst. Geol. Geofiz., Novosibirsk, 1987), pp. 130–144 [in Russian].
23. A. S. Gibsher and A. A. Terleev, "The Upper Precambrian–Lower Paleozoic Stratigraphy of the Sangilen Upland," in *Structural–Lithologic Complexes of the Southeastern Tuva* (Inst. Geol. Geofiz., Novosibirsk, 1989), pp. 3–26 [in Russian].
24. S. J. Goldstein and S. B. Jacobsen, "Nd and Sr Isotopic Systematics of Rivers Water Suspended Material: Implications for Crustal Evolution," Earth Planet. Sci. Lett. **87**, 249–265 (1988).
25. V. E. Gonikberg, "Paleotectonic Nature of the Northwestern Margin of the Sangilen Massif (Tuva) in the Late Precambrian," Geotektonika, No. 5, 72–84 (1997) [Geotectonics **31**, 408–419 (1997)].
26. P. F. Hoffman, "Did the Breakout of Laurentia Turn Gondwanaland Insides-Out?," Science **252**, 1409–1412 (1991).
27. A. V. Il'in, "Stratigraphy of Precambrian Deposits in the Western Sangilen (Tuva)," Sov. Geol., No. 4, 33–42 (1958).
28. A. V. Il'in, "Geologic Evolution of Southern Siberia and Mongolia in the Late Precambrian–Cambrian" (Nauka, Moscow, 1982) [in Russian].
29. S. B. Jacobsen and G. J. Wasserburg, "Sm-Nd Evolution of Chondrites and Achondrites. II," Earth Planet. Sci. Lett. **67**, 137–150 (1984).
30. L. S. Keto and S. B. Jacobsen, "Nd and Sr Isotopic Variations of Early Paleozoic Oceans," Earth Planet. Sci. Lett. **84**, 27–41 (1987).
31. E. V. Khain, E. V. Bibikova, A. Kröner, *et al.*, "The Most Ancient Ophiolite of the Central Asia Fold Belt: U–Pb and Pb–Pb Zircon Ages for the Dunzhugur Complex, Eastern Sayan, Siberia, and Geodynamic Implications," Earth Planet. Sci. Lett. **199**, 311–325 (2002).
32. T. N. Kheraskova, A. N. Didenko, V. A. Bush, and Yu. A. Volozh, "The Vendian-Early Paleozoic History of the Continental Margin of Eastern Paleogondwana, Paleoasian Ocean and Central Asian Foldbelt," Rus. J. Earth Sci **5** (3), 165–184 (2003).
33. T. I. Kirnozova, E. V. Bibikova, I. K. Kozakov, *et al.*, "Early Proterozoic Post-Collision Granitoids in the Near-Sayan Basement Ledge of the Siberian Platform: U–Pb Geochronological and Sm–Nd Isotopic Data," in *Proceedings of the II Russian Conference on Isotopic Geochronology, St. Petersburg* (Tsentr Inform. Kul'tury, St. Petersburg, 2003), pp. 193–195 [in Russian].
34. A. B. Kotov, V. P. Kovach, E. B. Sal'nikova, *et al.*, "Age and Formation Stages of Continental Crust in the Central Aldan Granulite–Gneiss Area: U–Pb and Sm–Nd Isotopic Data on Granitoids," Petrologiya **3** (1), 97–108 (1995)
35. A. B. Kotov, E. B. Sal'nikova, V. P. Kovach, *et al.*, "Age of Metamorphism of the Slyudyanka Crystalline Complex, Southern Baikal Area: U–Pb Geochronology of Granitoids," Petrologiya **5**, 380–393 (1997) [Petrology **5**, 338–349 (1997)].
36. V. P. Kovach, A. B. Kotov, A. P. Smelov, *et al.*, "Evolutionary Stages of the Continental Crust in the Buried Basement of the Eastern Siberian Platform: Sm–Nd Isotopic Data," Petrologiya **8**, 394–408 (2000) [Petrology **8**, 353–365 (2000)].
37. V. I. Kovalenko, V. V. Yarmolyuk, V. P. Kovach, *et al.*, "Sources of Phanerozoic Granitoids in Central Asia: Sm-Nd Isotope Data," Geokhimiya, No. 8, 699–712 (1996) [Geochem. Int. **34**, 628–640 (1996)].
38. V. I. Kovalenko, V. V. Yarmolyuk, V. P. Kovach, *et al.*, "Magmatism as Factor of Crust Evolution in the Central Asian Foldbelt: Sm–Nd Isotopic Data," Geotektonika, No. 3, 21–41 (1999) [Geotectonics **33**, 191–208 (1999)].
39. V. I. Kovalenko, V. V. Yarmolyuk, V. P. Kovach, *et al.*, "Magmatism and Geodynamics of Early Caledonian Structures in the Central Asian Foldbelt (Isotopic and Geochronological Data)," Geol. Geofiz. **44**, 1280–1293 (2003).
40. I. K. Kozakov, *Precambrian Infracrustal Complexes of Mongolia* (Nauka, Leningrad, 1986) [in Russian].
41. I. K. Kozakov, A. B. Kotov, V. P. Kovach, and E. B. Sal'nikova, "Crustal Growth in the Geologic Evolution of the Baidarik Block, Central Mongolia: Evidence from Sm–Nd Isotopic Systematics," Petrologiya **5**, 240–248 (1997a) [Petrology **5**, 201–207 (1997)].
42. I. K. Kozakov, A. B. Kotov, V. P. Kovach, and E. V. Sal'nikova, "Crustal Growth in Geologic Evolution of the Dzabkhan and Tuva–Mongolian Microcontinents in the Central Asian Foldbelt: U–Pb and Sm–Nd Isotopic Data," in *Tectonics of Asia* (GEOS, Moscow, 1997) [in Russian].
43. I. K. Kozakov, A. B. Kotov, E. B. Sal'nikova, *et al.*, "Metamorphic Age of Crystalline Complexes of the Tuva-Mongolia Massif: The U–Pb Geochronology of Granitoids," Petrologiya **7**, 173–189 (1999) [Petrology **7**, 177–191 (1999)].
44. I. K. Kozakov, A. B. Kotov, E. B. Sal'nikova, *et al.*, "Timing of the Structural Evolution of Metamorphic Rocks in the Tuva-Mongolian Massif," Geotektonika, No. 3, 22–43 (2001) [Geotectonics **35**, 165–184 (2001)].
45. I. K. Kozakov, V. I. Kovalenko, and V. V. Yarmolyuk, "The Late Riphean Crustal Grows and Isotopic Structure of Central Asia," in *Proceedings of the XXXVII Tectonic Conference: Evolution of Tectonic Processes in the Earth's History* (Geo, Novosibirsk, 2004) [in Russian].

46. I. K. Kozakov, V. P. Kovach, V. V. Yarmolyuk, *et al.*, "Crust-Forming Processes in the Geologic Development of the Tuva-Mongolia Massif: Sm–Nd Isotopic and Geochemical Data for Granitoids," Petrologiya **11**, 491–512 (2003) [Petrology **11**, 444–463 (2003)].
47. I. K. Kozakov, E. B. Sal'nikova, E. V. Khain, *et al.*, "Early Caledonian Crystalline Rocks of the Lake Zone in Mongolia: Formation History and Tectonic Settings as Deduced from U-Pb and Sm-Nd Dating," Geotektonika, No. 2, 80–92 (2002) [Geotectonics **36**, 156–166 (2002)].
48. A. Kröner, G.W. Zhang, and Y. Sun, "Granulites in the Tongbai area, Qinling Belt, China: Geochemistry, Petrology, Single Zircon Geochronology and Implications for the Tectonic Evolution of Eastern Asia," Tectonics, No. 2, 139–166 (1993).
49. A. B. Kuzmichev, "Analogues of the Vendian–Cambrian Bokson Group in the Northeastern Tuva–Mongolian Massif," Izv. Vyssh. Uchebn. Zaved., Geol. Razved., No. 3, 330–344 (1994).
50. A. B. Kuzmichev, "Tectonic Implication of the Paleozoic Granite Magmatism in the Baikalides of the Tuva-Mongolian Massif," Geotektonika, No. 6, 76–92 (2000) [Geotectonics **34**, 497–511 (2000)].
51. A. B. Kuzmichev, *Tectonic History of the Tuva–Mongolian Massif: Early to Late Baikalian and Early Caledonian Stages* (PROBEL, Moscow, 2004) [in Russian].
52. A. B. Kuzmichev, E. V. Bibikova, and D. Z. Zhuravlev, "Neoproterozoic (~800 Ma) Orogeny in the Tuva-Mongolia Massif (Siberia): Island Arc–Continent Collision at the North-East Rodinia Margin," Precambrian Res. **110**, 109–126 (2001).
53. A. B. Kuznetsov, M. A. Semikhatov, I. M. Gorokhov, *et al.*, "Sr Isotope Composition in Carbonates of the Karatau Group, Southern Urals, and Standard Curve of $^{87}Sr/^{86}Sr$ Variations in the Late Riphean Ocean," Stratigr. Geol. Korrelyatsiya **11** (5), 3–39 (2003) [Stratigr. Geol. Correlation **11**, 415–449 (2003)].
54. A. B. Kuzmichev, D. Z. Zhuravlev, E. V. Bibikova, and T. I. Kirnozova, "The Late Riphean (790 Ma) Granitoids of the Tuva–Mongolian Massif: Evidence in Favor of the Early Baikalian Orogenesis," Geol. Geofiz. **41** (10), 1379–1383 (2000).
55. E. F. Letnikova, "Geochemical Characteristics of Carbonate Rocks as Indicators of Paleogeodynamic Settings," Dokl. Akad. Nauk **385**, 672–676 (2002) [Dokl. Earth Science **385A** (6), 710–713 (2002)].
56. Z. X. Li, X. H. Li, P. D. Kinny, *et al.*, "Geochronology of Neoproterozoic Syn-Rift Magmatizm in Yangtze Craton, South China and Correlations with Other Continents: Evidence for a Mantle Super Plume that Broke Up Rodinia," Precambrian Res. **122**, 85–109 (2003).
57. Yu. M. Mal'tsev and N. V. Mezhelovskii, "New Data on Riphean Biostratigraphy of the Sangilen," in *Stratigraphy of the Precambrian and Cambrian in Central Siberia* (Inst. Geol. Geofiz., Krasnoyarsk, 1967), pp. 376–380 [in Russian].
58. S. Maruyama, "Plume Tectonics," J. Geol. Soc. Japan **100** (1), 24–49 (1994).
59. S. M. McLennan, S. Hemming, D. K. McDaniel, and G. N. Hanson, "Geochemical Approaches to Sedimentation, Provenance and Tectonics," Spec. Pap. Geol. Soc. Am., No. 284, 21–40 (1993).
60. F. P. Mitrofanov, I. K. Kozakov, and I. P. Palei, *The Precambrian of Western Mongolia and Southern Tuva* (Nauka, Leningrad, 1981) [in Russian].
61. A. A. Mossakovskii, S. V. Ruzhentsev, S. G. Samygin, and T. N. Kheraskova, "The Central Asian Foldbelt: Geodynamic Evolution and Formation History," Geotektonika, No. 6, 3–32 (1993).
62. A. N. Neelov, *Petrochemical Classification of Metasedimentary and Metavolcanic Rocks* (Nauka, Leningrad, 1980) [in Russian].
63. P. J. Patchett, "Isotopic Studies of Proterozoic Crustal Growth and Evolution," in *Proterozoic Crustal Evolution*, Ed. by K.C. Condie (Elsevier, Amsterdam, 1992), pp. 481–508.
64. V. N. Podkovyrov, I. K. Kozakov, V. P. Kovach, *et al.*, "The Siberian Craton in Structures of Proterozoic Supercontinents," in *Supercontinents in Precambrian Geologic Evolution* (Inst. Zemnoi Kory, Irkutsk, 2001), pp. 193–196 [in Russian].
65. R. H. Rainbird, R. A. Stern, A. K. Khudoley, *et al.*, "U–Pb Geochronology of Riphean Sandstone and Gabbro from Southeast Siberia and Its Bearing on the Laurentia-Siberia Connection," Earth Planet. Sci. Lett. **164**, 409–420 (1998).
66. *The Early Precambrian of Central Asian Foldbelt*, Ed. by I. K. Kozakov (Nauka, St. Petersburg, 1993) [in Russian].
67. J. C. Roddick and O. van Breemen, "U–Pb Zircon Dating: A Comparison of Ion Microprobe and Single Grain Conventional Analyses," in *Radiogenic age and Isotopic Studies, Report 8* (Geol. Surv. Can., 1994), pp.1–9.
68. J. J. W. Rogers, "A History of Continents in the Past Three Billion Years," J. Geol. **104**, 91–107 (1996).
69. J. J. W. Rogers and M. Santosh, "Configuration of Columbia, a Mesoproterozoic Supercontinent," Gondwana Res. **5** (1), 5–22 (2002).
70. J. J. W. Rogers and M. Santosh, "Supercontinents in Earth History," Gondwana Res. **6** (3), 357–368 (2003).
71. O. M. Rozen, "Graywackes in Precambrian Metamorphic Complexes (Relationships between Composition and Geodynamic Settings)," Izv. Vyssh. Uchebn. Zaved., Geol. Razved., No. 1, 36–50 (1993).
72. O. M. Rozen and V. S. Fedorovskii, *Collision Granitoids and the Earth Crust Delamination* (Nauchnyi Mir, Moscow, 2001) [in Russian].
73. S. V. Ruzhentsev and V. V. Burashnikov, "Tectonics of the Salairides in Western Mongolia," Geotektonika, No. 5, 25–40 (1995).
74. E. Yu. Rytsk, Yu. V. Amelin, N. G. Rizvanova, *et al.*, "Age of Rocks in the Baikal–Muya Foldbelt," Stratigr. Geol. Korrelyatsiya **9** (4), 3–15 (2001) [Stratigr. Geol. Correlation **9**, 315–326 (2001)].
75. E. B. Salnikova, I. K. Kozakov, A. B. Kotov, *et al.*, "Age of Palaeozoic Granites and Metamorphism in the Tuvino-Mongolian Massif of the Central Asian Mobile Belt: Loss of Precambrian Microcontinent," Precambrian Res. **110**, 143–164 (2001).
76. M. A. Semikhatov, "Refined Isotopic Ages of Lower Boundaries of the Upper Riphean, Vendian, and Cambrian," in *Addenda to the Stratigraphic Code of Russia* (VSEGEI, St. Petersburg, 2000), pp. 95–107 [in Russian].

77. M. A. Semikhatov and S. N. Serebryakov, "The Vendian and Lower Cambrian in the Southeastern East Sayan Mountains," Izv. Akad. Nauk SSSR, Ser. Geol., No. 4, 87–103 (1967).
78. M. A. Semikhatov and S. N. Serebryakov, *The Riphean Hypostratotype of Siberia* (Nauka, Moscow, 1983) [in Russian].
79. M. A. Semikhatov, A. B. Kuznetsov, I. M. Gorokhov, *et al.*, "Low $^{87}Sr/^{86}Sr$ Ratios in Seawater the Grenville and Post-Grenville Time: Determining Factors," Stratigr. Geol. Korrelyatsiya **10** (1), 3–46 (2002) [Stratigr. Geol. Correlation **10**, 1–41 (2002)].
80. A. M. J. Sengör, B.A. Natal'in, and V.S. Burtman, "Tectonic Evolution of the Altaides," Geol. Geofiz. **35** (7–8), 41–58 (1994).
81. R. H. Steiger and E. Jaeger, "Subcommission of Geochronology: Convention of the Use of Decay Constants in Geo- and Cosmochronology," Earth Planet. Sci. Lett. **36** (2), 359–362 (1976).
82. S. R. Taylor and S. M. McLennan, *The Continental Crust: Its Composition and Evolution* (Blackwell Scientific Publications, Oxford, 1985).
83. *Tectonic Map of Northern Eurasia, Scale 1 : 5000000* (GUGK, Moscow, 1979) [in Russian].
84. *The Precambrian of East Sayan Mountains* (LAGED, Leningrad, 1964) [in Russian].
85. A. F. Veis and N. G. Vorob'eva, "The First Finds of Organic-Walled Microfossils in the Upper Precambrian of the Bokson–Sarkhoi Depression (the Eastern Sayan)," Stratigr. Geol. Korrelyatsiya **1** (4), 27–32 (1993) [Stratigr. Geol. Correlation **1**, 393–405 (1993)].
86. A. E. Vernikovskaya, V. L. Pease, V. A. Vernikovsky, *et al.*, "Geochemistry and Petrology of Neoproterozoic Granites of the Mamont-Shrenk Terrane, Central Taimyr," Geokhimiya, No. 5, 486–498 (2002) [Geochem. Int. **40**, 435–446 (2002)].
87. A. E. Vernikovskaya, V. A. Vernikovsky, E. B. Sal'nikova, *et al.*, "Granitoids of the Eruda and Chirimba Massifs, Trans-Angara area of the Yenisei Range, as Indicators of Neoproterozoic Collision Events," Geol. Geofiz. **43** (3), 259–272 (2002a).
88. V. A. Vernikovsky, A. E. Vernikovskaya, A. I. Chernykh, *et al.*, "Porozhnaya Granitoids of the Enisei Ophiolite Belt: Indicators of Neoproterozoic Events on the Enisei Ridge," Dokl. Akad. Nauk **381** (6), 806–810 (2001) [Dokl. Earth Science **381A** (9), 1043–1046 (2001)].
89. V. A. Vernikovsky, A. E. Vernikovskaya, E. B. Sal'nikova, *et al.*, "Postcollision Granitoid Magmatism in the Transangara Region of the Yenisei Range: An Event 750–720 Ma B.P.," Dokl. Akad. Nauk **384** (2), 221–226 (2002) [Dokl. Earth Science **384** (4), 362–366 (2002)].
90. V. A. Vernikovsky, V. P. Kovach, A. B. Kotov, *et al.*, "Sources of Granitoids and the Evolutionary Stages of the Continental Crust in the Taimyr Folded Area," Geokhimiya, No. 6, 563–573 (1999) [Geochem. Int. **37**, 493–502 (1999)].
91. T. Wang, Ya. Zheng, G. E. Gehrels, and Z. Mu, "Geochronological Evidence for Existence of South Mongolian Microcontinent—A Zircon U–Pb Age of Granitoid Gneisses from the Yagan-Onch Hayrhan Metamorphic Core Complex," Chinese Sci. Bull **46** (23), 2005–2008 (2001).
92. F. Xue and M. F. Lerch, A. Kröner, and T. Reischmann, "Tectonic Evolution of the East Qinling Mountains, China, in the Paleozoic: a Review and New Tectonic Model," J. South Am. Earth Sci. **253**, 271–284 (1996).
93. V. V. Yarmolyuk and V. I. Kovalenko, "Late Riphean Breakup between Siberia and Laurentia: Evidence from Intraplate Magmatism," Dokl. Akad. Nauk **379** (1), 94–98 (2001) [Dokl. Earth Science **379** (5), 526–528 (2001)].
94. V. V. Yarmolyuk and V. I. Kovalenko, "Deep Geodynamics and Mantle Plumes: Their Role in the Formation of the Central Asian Fold Belt," Petrologiya **11**, 556–586 (2003) [Petrology **11**, 504–531 (2003)].
95. V. V. Yarmolyuk, V. I. Kovalenko, V. P. Kovach, *et al.*, "Geodynamics of Caledonides in the Central Asian Foldbelt," Dokl. Akad. Nauk **389** (3), 354–359 (2003) [Dokl. Earth Science **389A** (3), 311–316 (2003)].
96. V. V. Yarmolyuk, V. I. Kovalenko, V. P. Kovach, *et al.*, "Nd-Isotopic Systematics of Western Transbaikalian Crustal Protoliths: Implications for Riphean Crust Formation in Central Asia," Geotektonika, No. 4, 3–20 (1999) [Geotectonics **33**, 271–286 (1999)].
97. M. Zhai, Ji. Sao, Ji. Hao, and P. Peng, "Geological Signature and Possible Position of the North China," Gondwana Res. **6** (2), 171–183 (2003).
98. L. P. Zonenshain and M. I. Kuz'min, *Paleogeodynamics* (Nauka, Moscow, 1993) [in Russian].
99. L. P. Zonenshain, M. I. Kuz'min, and L. M. Natapov, *Plate tectonics of the USSR Territory* (Nedra, Moscow, 1990) [in Russian].